APPENDIX 2P

SEABROOK STATION CONTAINMENT AIRCRAFT IMPACT ANALYSIS

The information contained in this appendix was not revised, but has been extracted from the original FSAR and is provided for historical information.

APPENDIX 2P

SEABROOK STATION CONTAINMENT

AIRCRAFT IMPACT ANALYSIS

Prepared by

UNITED ENGINEERS
& CONSTRUCTORS INC.

OCTOBER 1975

PUBLIC SERVICE COMPANY OF NEW HAMPSHIRE
SEABROOK, NEWHAMPSHIRE

CONTENTS

ABSTRACT

Results are presented which verify the adequacy of the Seabrook containment to resist the impact of an FB-111 type aircraft. Included is a description of the dynamic forcing function, the elastic-dynamic analysis, the elastic-plastic analysis, an estimate of reinforcement and liner strain and a verification of the punching shear capability of the containment.

It is shown that there exists no credible mechanism by which spilled fuel from the impacting aircraft can access the annulus. The ensuing fire is, therefore, postulated to start in the immediate vicinity external to the enclosure and it is demonstrated that these external fires do not, in any way, inhibit or handicap the safe shutdown capability of the plant following the postulated crash.

It is concluded, that under the aircraft impact, the containment structure is able to withstand postulated impact and that the consequences of the aforementioned fire hazard is mitigated by the inherent design features of Seabrook Station.

1.0 STRUCTURAL ANALYSIS OF SEABROOK STATION CONTAINMENT FOR AIRCRAFT IMPACT

1.1 Introduction

The Seabrook Station containment has been analyzed for the effects of a-postulated impact by an FB-111 type aircraft with a speed at impact of 200 mph. Based on the analyses performed;-the adequacy of the containment to withstand the postulated impact is verified. The Seabrook Station containment and enclosure building is described in Section 3.8.1 of the Seabrook PSAR. The FB-111 aircraft, the missile in the postulated impact,is 73.5 feet long, has a wingspan (spread oosition) of 70.0 feet and weighs 81.800 Dounds (See Reference 1).

In order to perform the analyses, a force-time relationship is developed from the mechanical properties of the impacting aircraft. An elastic dynamic analysis indicates that an elastic-plastic dynamic analysis is required to predict the flexural response of the structure. From this analysis of the structure, an estimate is made of the strains experienced by the reinforcing bars and liner. Subsequently, an analysis is performed to verify the adequacy of the containment against punching shear and penetration.

1.2 FORCING FUNCTION FOR IMPACTING AIRCRAFT

The time variation of the load on a rigid surface due to an impacting aircraft may be developed using the momentum principle. The governing equations which are used to determine the time variation of the force experienced by the target are (Reference 2):

$$-P_c(\zeta_n(t)) = \frac{d^2\zeta_n}{dt^2} \int_{\zeta_n(t)}^{L} \omega(x,t)\, dx$$

$$R(t) = P_c(\zeta_n(t)) + \left(\frac{d\zeta_n}{dt}\right)^2 \omega(\zeta_n,t)$$

where

R(t) is the force acting on the target (positive for compression),

$\xi_n(t)$ is the extent of crushing at any time t as measured from the leading edge of nose of the missile,

$P_c(\xi_n)$ is the load required to crush the cross section of the missile at any distance ξ_n from the nose, (positive for compression)

$\omega(\xi_n)$ is the mass density per unit length of the missile as a function of the distance from the nose.

These equations are used to determine the two unknowns, the crushing length, $\xi_n(t)$, and the reaction, R(t), as functions of time. The information required to determine these variables consists of the initial impact velocity, weight or mass distribution and crushing load distribution of the aircraft.

The first equation is integrated numerically to obtain the velocity time history. The reaction force is then determined from the second equation.

Figure 1 shows three views of the FB-111 aircraft. Figure 2a shows the one dimensional idealized model of the same aircraft. Figure 2b describes the weight distribution for an FB-111 with a total weight of 81,800 pounds. The sketch and the weight distribution are obtained from Reference 1. The particular configuration used is essentially the same as that summarized on P. 1.3.3 of Reference 1 with the wing stores and wing useful load removed.

This configuration is consistent with the normal operation (90% of the time) of the FB-111 at Pease AFB. The value of 81,800 pounds is the

weight before the airplane has warmed up and taken off. In normal flights the aircraft would fly a mission and return to Pease AFB with approximately 10,000 pounds of fuel. On this basis, the landing weight would be approximately 59,000 pounds. For those missions when the aircraft is flown with wing tanks the maximum take-off weight is 100,000 pounds. The FB-lllis not allowed to land with fuel in these wing tanks; therefore in all cases the maximum landing weight is 81,800 pounds.

Thus, the 81,800 lbs weight of the FB-111 used in the impact analysis was the fully loaded FB-111 without wing tanks. This weight is conservatively large for any configuration of the aircraft flying out of Pease AFB, but it was used because it represented a maximum upper bound on the weight of the FB-111 in the landing pattern.

The exact crushing load distribution for an PB-111 is not available. The crushing load distribution shown on Figure 2c is arrived at by scaling the known values for a Boeing-720(Ref.2).It is demonstrated in this report that the peak value of the reaction is relatively insensitive to reasonable variations of the crushing load.

Figure 3 shows the reaction-time relationship for the FB-111 striking a rigid wall at an impact velocity of 200 mph. The peak value of the reaction is 8.2 x 10^6 pounds. This peak value occurs when the wing structure is in the process of collapsing. This peak reflects the

concentration of mass in the wing structure and the fuel that is stored in the fuselage in the vicinity of the wing location. It is noted that the cross-sectional area over which the peak occurs will be considerably larger than the area of fuselage cross-section. The secondary peak of 4.2 x 10^6 pounds (at 0.21 sec.) occurs when the airplane is crushing in the vicinity of the engines.

The determination of the sensitivity of the reaction to the magnitude of the crushing load is investigated by determining the reaction for values of one-fifth and five times this crushing load. These results are shown in Figure 4. From Figure 4, the peak values of the reactions are:

Pc/5	8.5 x 10^6 pounds
PC	8.2 x 10^6 pounds
5xP_c	7.1 x 10^6 pounds

The peak value of the reaction is relatively insensitive to variations in the magnitude of the crushing load, and the scaled value of Pc is judged to give accurate results.

1.3 Flexural Behavior of Containment

1.3.1 Elastic Dynamic Analysis

For the elastic dynamic analysis, the finite element method was chosen as the analytical method, and a computer program for axisymmetric structures subjected to arbitrary static and dynamic loads was used. (See Reference 3 for the basis of the mechanics of the program.) Damping was not considered. Thus, the predicted structural response is slightly larger than that which does occur.

To accomplish the analysis, several assumptions were made. They are as follows:

i) The containment is fixed at the base of the cylinder.

ii) Impact loads are uniformly distributed over the loading zones.

iii) In the axisymmetric analysis (impact at apex of dome), the loading zone is a circle with a radius of 52.77 inches and an area of 8748.3 square inches.

iv) In the asymmetric analysis (impact at springline), the loading zone is a square, 93.53 inches on a side and 8748.3 square inches in area.

v) The stiffness of the reinforcing steel is neglected; only the gross concrete volume is considered. The modulus of elasticity was taken as 3.0×10^6 lbs/sq. in., Poisson's ratio was taken as 0.15, and the weight density was taken as 150 pcf.

vi) The effect of the enclosure building is neglected. It can be shown that the enclosure absorbs approximately 4% of the energy of the impacting aircraft.

The containment structure is modeled with axisymmetric conical shell elements, a plot of this model is shown in Figure 5.

Two impact positions, the apex of the dome and the springline, are considered. The impact at the dome is uniformly distributed over the first seven (7) elements, and the impact at the springline is uniformly distributed over the six (6) elements nearest to the springline. By means of a half-range cosine series, the load at the springline is confined to a

6.18' arc. Thirty (30) terms were used to represent this Fourier series which is shown, normalized to 1.0, in Figure 6. Experience with loadings similar to the loadings here, has demonstrated that twenty (20) terms of the series were found to be too few and ninety (90) terms were found to yield results very close to those generated by thirty (30) terms.

Selected maximum results for the axisymmetric and asymmetric analyses are given in Tables 1-1 and 1-2, respectively. These moments will cause cracking of the concrete and yielding of the rebar. Therefore, an elastic-plastic dynamic analysis is required.

1.3.2' Elastic-Plastic Dynamic Analysis

The procedure followed for the elastic-plastic analysis of the response of the containment under aircraft impact follows that of Biggs (Reference 4). In this procedure, knowing the load-time relationship, the first natural frequency of that part of the structure participating in the energy absorption, and the allowable ductility ratio (defined as the ratio of the maximum deflection to the deflection at yield), the ratio (F/Rm) of the maximum value of the load-time relationship to the maximum value of the resistance function can be determined. This

can then be compared with the actual estimated maximum values of the load-time relationship and resistance function.

The force-time relationship, given in Figure 3 is approximated by a triangular load-time curve with the same total impulse and peak force. This ideal and the actual force-time relationships are compared in Figure 7 . It is assumed that a circular region of radius "a" will participate in the energy absorption. The natural frequency, associated with this participating region, is estimated on the basis of the first natural frequency of a flat circular plate of radius "a" clamped at the edges. The assumption of clamped edges, in that it gives a smaller period for the first natural frequency than in the actual case, is a conservative simplification. This follows because, in general the value of the maximum allowable forcing function decreases as the first natural period decreases (Ref. 4, p. 78, Figure 2.26). Conversely, ignoring the curvature is non-conservative in that it gives an estimate of the period which is larger than the actual case. For small values of the radius "a", the curvature effect is minimal.

All calculations are based upon the 3'-6" dome section configuration. The first natural frequency of a flat circular plate, clamped at the edge is:

$$P = \sqrt{\frac{D}{M}}\ \frac{1}{a^2} \quad X.17$$

where D is the flexural rigidity and M is the mass density per unit surface area (See, for example, Ref. 5).

For the 3'-6" thick concrete plate with a Young's modulus of 3×10^6 psi and a unit weight of 150 pounds per cubic foot, the period is:

uncracked section $T = \frac{a^2}{15.94 \times 10^3}$ "a" in feet

cracked section $T = \frac{a^2}{12.86 \times 10^3}$

Using Fig, 2.26 of Reference 4 (p. 78), the ratio F/Rm, as a function of the radius of the participating material of the containment, can be determined for various values of ductility ratio.

For the purpose of this investigation, two (2) ductility ratios, 3 and 10 are used. For plates and shells, the lower value is conservative, the larger value reasonable. The results of the calculations are shown in Table 1-3 and Figure 8. Although the range of Fig. 2.26 of Reference 4 is limited to a td/T of 20, it can be observed that for a ductility ratio greater than two and td/T of 20, F/Rm is greater than unity. Therefore, the allowable peak force, F, can be larger than the maximum value of the resistance, Rm.

1.3.3 Resistance Function

In the vicinity of the impact region, the response of the structure is assumed to have the characteristics shown in Figure 9a.

For values of the force less than Rm, the displacements are limited in magnitude even though the response may be inelastic. As the load reaches the value Rm, the deformations are able

to become arbitrarily large, i.e., the collapse load has been reached. The collapse load for a concentrated load on a curved shell is not readily accessible. As a conservative estimate, the collapse load for a flat plate with reinforcement the same as the dome is used to estimate the collapse load for the shell..

Expecting the yield line formation shown in Figure **9b** observation suggests that the clamped boundary condition case should be used. The value of the collapse load, Rm, is then (Reference **6)**

$$R_M = 2\pi(M_u^+ + M_u^-)$$

where M_u is the ultimate moment capacity and the notation + and - refers to the outside and inside reinforcement respectively.

The ultimate moment capacities and collapse loads of the containment are:

dome $M^+ = 643$ k-ft./ft.
$M^- = 651$ k-ft./ft.
Rm = 8,131k

springline $M^+ = 1,235$ k-ft./ft
M- = 643 k-ft./ft
Rm = 11,800k

At the dome, the collapse load and peak load are approximately equal. However, from Figure 8 , the dynamic effect allows the structure to withstand loads in excess of the capacity. From Figure **8** the allowable load is 10% larger than the resistance or collapse load. Therefore, the apex will not

collapse. Since the maximum load, 8,200k is less than the capacity of the dome in the springline, 11,800k, collapse will not occur at the springline.

The dome will not collapse, under the applied load.

1.3.4 Estimation of Rebar and Liner Strains

While plastic analysis techniques are useful for finding collapse loads, they cannot be directly used to find the strains and displacements corresponding to collapse loads.

However, a procedure making use of the ductility ratio can be used to approximate the maximum strains in the structure subject to dynamic loading when nonlinear material behavior is encountered. This procedure is described below.

A typical load-displacement curve for reinforced concrete section is shown in Figure 10. This curve is linear up to the load causing cracking (P_{cr}) after which a straight line of somewhat flatter slope is obtained until the load (P_y) is reached which causes yielding of the steel.

Any increase in load beyond (P_y) causes the displacement to increase disproportionately. Further increase in load causes extensive displacements to occur, resulting in eventual collapse. This actual behavior of the structure was idealized as shown in Figure 9a, and was used for the elastic-plastic dynamic analysis previously discussed. This idealized curve represents the resistance function of the structure.

The ductility ratio, μ, referred to in the elastic-plastic dynamic analysis represents the ratio of the maximum displacement of the structure to the deflection established as yield (Y_{el}) for the structure.

While it is recognized that the ductility ratio is not an exact measure of the maximum strain at a particular point of the structure, it can be used as an approximation because the strain at yield in the actual structure is very nearly the strain corresponding to yield for the idealized structure.

The procedure used herein is based on the peak of the actual forcing function resulting from the-aircraft impact, the duration of loading, the idealized resistance function for the structure and the first natural period of the responding part of the structure. By using the above known quantities, the corresponding ductility ratio for the structure may be determined.

For a peak in the forcing function of 8,200k and a maximum force in the resistance function of 8,130 k, the maximum ductility ratio for all ratios of t_d/T is approximately 1.5 (See Fig. 2-26, Ref. 2). Thus, regardless of the natural period of the responding part of the structure, the largest displacement that will occur under the aircraft impact loading is the same as that corresponding to yield for the idealized structure.

The yield strain for the reinforcing steel is

$$\varepsilon_Y = \frac{60}{30 \times 10^3} = 0.002 \text{ in/in}$$

If it is assumed that the strain corresponding to yield (Y_{el}) for the idealized structure is 50% larger than this (actually is much less than this),, then an upper bound for the strain in the reinforcing steel will be:

$$\varepsilon = 1.5 \times 1.5 \times 0.002 \text{ in/in} = 0.0045 \text{ in/in}$$

Since the liner and the tension reinforcing steel are only several inches apart in a 42" thick containment dome, they will be strained to nearly the same values. Hence, there will be no possibility of impairing the leak tight integrity of the liner.

1.4 Response of the Enclosure Building

During the early stages of the impact process, the enclosure building will deform until it comes into contact with the containment. The enclosure building must deflect five feet in order to come into contact with the containment dome. Such a deformation will involve an inelastic response. This inelastic response will involve both flexure and shear.

The 15" thick enclosure building is reinforced with #10's @ 12", both ways and both faces. The collapse load is 635k.

The allowable shear load will depend upon the shear area over which the transverse shear stress acts. This shear area is determined by multiplying the average shear periphery by the effective depth of the shell. The average shear periphery is determined by a contour which is at a distance of one-half the effective depth away from the contour of the contact area (Figure 11). Figures 12 to 21 show the impact area and shear periphery associated with various locations

along the aircraft and for the effective depths of the enclosure building (9") and containment (37").

The reaction as a function of the cross section being crushed is determined from the reaction-time and crushing distance relationship and is shown in Figure 22.

From this information, it is possible to examine the effect of the aircraft impact on the enclosure building as a function of the distance being crushed. Figure 23 shows the average shear stress on the enclosure as a function of distance being crushed. For example, using a shear strength of $4.25\sqrt{f'_c}$, the enclosure building will fail by shear when the aircraft is crushing at 7.25 feet. Also shown on Figure 23 is the reaction as a function of the distance being crushed. For a collapse load of 635k, the enclosure building will collapse when the aircraft is crushing at 9.75 feet. It would appear that, using $4.25\sqrt{f'_c}$ as a shear strength, the enclosure building would fail by shear before collapse, however, the two events would occur at a time difference of 0.0086 sec. Any increase in actual shear strength above $4.25\sqrt{f'_c}$ would increase the possibility of punch through and collapse happening simultaneously. As will be domonstrated in Section 1.5, the actual shear strength can vary considerably above a value of $4.25\sqrt{f'_c}$. No clear conclusion can be drawn as to whether punch through or collapse occurs first. Based on the above discussion, the failure of the enclosure building will involve both extensive shear and flexure damage and it will deform until it comes into contact with the containment.

1.5 Shear Capability of the Containment

The enclosure building will deform until it comes into contact with the containment dome. The dome will then resist the impact force and experience transverse shear stress in the vicinity of the impact area. The maximum average shear stress is determined by defining a shear perimeter and thickness over which the impact force is acting. Figure 24 describes the procedure by which the shear perimeter for the maximum average shear stress acting on the containment dome is determined. The shear perimeter for the containment is at a distance

$$\text{(effective depth of enclosure)} + \left(\frac{\text{effective depth of containment}}{2}\right)$$

away from the perimeter of the impact area.

The values of the shear perimeter for various cross sections of the aircraft are given in Table 1-4. Also shown are the shear area, impact force and average shear stress for the containment building. The values of average shear stress as a function of the cross section being crushed is shown in Figure 25. The shear stress is given in terms of psi and $\sqrt{f'_c}$. The maximum value of the average shear stress occurs when the aircraft is crushing at a distance of 35 feet from the nose. The value of this maximum average shear stress is 229 psi or $4.18\sqrt{f'_c}$.

Various shear strengths have been proposed. A tabulation of these shear strengths, for parameters similar to the aircraft and structure under discussion is shown in Table 1-5. It is seen that the maximum nominal shear stress of $4.18\sqrt{f'_c}$ is less than all the other proposed values except the conservative value of $4\sqrt{f'_c}$ as proposed by the

XI-Committee 326. Hence, it is concluded the the containment will not fail by punch through.

1.6 Requirements to Prevent Perforation

The velocity of the engines as they impact on the enclosure building and containment is 250 fps.

The FB-111 has two Pratt & Whitney **JTF10A-270** (Military designation **TF30-P-7)** jet turbo fan engines with an outside diameter of 50.22 inches. Each engine has a dry weight of 4,121 pounds (Ref. 1). The thickness of the dome required for no performation was determined using procedures reported in Reference 7.

The pertinent nomenclature is :

x	penetration thickness for infinitely thick slab (inches)
e	perforation thickness for reinforced concrete (inches)
dm	diameter of missile (inches)
v	velocity of impact (feet per second)
w	weight of missile
K	$\frac{180}{\sqrt{f'_c}}$
f'_c	ultimate compression strength of concrete (psi)

$$G = K(.72)(.50)\frac{W}{dm^3}\, dm^{0.2}\left(\frac{v}{1000}\right)^{1.8}$$

$$\frac{x}{dm} = 2\sqrt{G}, \quad G < 1.0$$

$$\frac{e}{dm} = 2.57\left(\frac{x}{dm}\right) - 0.454\left(\frac{x}{dm}\right)^2, \quad 0 \leq \frac{e}{dm} \leq 3$$

Since a jet engine is not completely solid (thin shells for torque transmission, blades for fan, compressor and turbine, burner cans for combustion) the engine was assumed to behave similarly to a hollow pipe missile.

For a fan-jet, the outside diameter is slightly larger than the gas generator. Two values of dm (the diameter of the gas generator) were used, SO.23 inches and 40 inches. The results are:

dm (inches)	e(inches)
50.22	21.8
40.00	22.8

These values can be compared with the dome thickness of 42 inches. From these calculations, it can be concluded that there will be no perforation.

1.7 Conclusions

From the above results of the analysis of the Seabrook Station Containment, the following conclusions can be made:

1. The enclosure building will fail and will come into contact with the containment building. The mode of failure will not be by shear or flexure alone, but will involve both types of damage.
2. The containment building will not fail. The flexural strength will prevent collapse. The shear strength will prevent.punch through. There will be permanent damage to the structure, but the extent of this damage will not be sufficient to cause loss of the integrity of the building.

3. The liner strains, although inelastic, will be sufficiently small so that tearing of the liner will not occur.
4. The engines will not perforate the containment.

These conclusions can be made even though the above analysis was performed with considerable conservatisms. The conservative aspects of the analysis are:

1. The reaction-time relationship was determined for impact on a rigid target. A realistic, flexible target would reduce the peak value of the reaction.
2. Normal impact was assumed. Any impact angle other than 90^{o} reduces the impact force and increase the area over which the impact force acts.
3. The arcing effect of the doubly-curved dome was ignored. Arching increases the collapse and punching load capacities.
4. The shear stresses can be computed more accurately using the effective force occuring during the time necessary for the structure to respond rather than the peak instantaneous force. The peak instantaneous force will give larger shear stresses than the effective force.
5. The actual concrete compression strength will be larger than the specified strength of 3,000 psi. This would result in a larger value for the shear strength.
6. A conservative estimate of the shear periphery used to calculate shear areas and shear strengths was chosen. The

failure cone was assumed to be through the containment only and not through the combined thicknesses of the containment and enclosure building, The latter would be more accurate.

The integrity of the containment building will not be impaired in the occurrence of the postulated aircraft impact.

1.8 REFERENCES FOR SECTION 1.0

1. "FB-111 Unit Inertia Data, "General Dynamics, Fort Worth Division, Report FZS-12-6010, Revision "A", January, 1968.

2. Riera, J.O., "On the Stress Analysis of Structures Subjected to Aircraft Impact Forces" Nuclear Engineering and Design, North Holland Publishing Company, Amsterdam, Holland, 8 (1968), p. 415-426.

3. Ghosh, S., and Wilson, E., "Dynamic Stress Analysis of Axisymmetric Structures Under Arbitrary Loading", University of California, Berkeley, CA., Revised Sept., 1975.

4. Biggs, J. M., Introduction to Structural Dynamics, McGraw-Hill, Inc., 1964, pps. 69-84.

5. Meiorovitch, Analytical Methods in Vibrations, The Macmillan Company, 1967, p. 183.

6. Save and Massonnet, Plastic Analysis and Design of Plates, Shells and Disks, North Holland, 1972, p. 245.

7. Kennedy, Effects of an Aircraft Crash Into a Concrete Reactor Containment Building. Holmes & Narver, Inc., July, 1966.

TABLE 1-1

MAXIMUM RESPONSE

AXISYMMETRIC ANALYSIS

(IMPACT AT DOME)

Moments	Meridional	-1006 Ft-K/Ft
	Circumferential	-1005 FT-K/FT
Forces	Meridional	-478 K/Ft
	Circumferential	-478 F/Ft

TABLE 1-2

MAXIMUM RESPONSE

ASYMMETRIC ANALYSIS

(IMPACT AT SPRINGLINE)

ELEMENT 36	Moments	Meridional	-1139 Ft-K/Ft
		Circumferential	-1309 **Ft-K/Ft**
	Forces	Meridional	383 **K/Ft**
		Circumferential	442 **K/Ft**
ELEMENT 37	Moments	Meridional	-1148. Ft-K/Ft
		Circumferential	1350 **Ft-K/Ft**
	Forces	Meridional*	378 **K/Ft**
		Circumferential	431 **K/Ft**

* Element 36 is element **immediately** above springline.

Element 37 is element immediately below springline.

TABLE 1-3

ALLOWABLE MAXIMUM FORCE, MAXIM?? RESISTANCE RATIO FOR VARIOUS DUCTILITY RATIOS AND PARTICIPATING TARGET MATERIAL RADII

A* (ft)	T (sec)	td/T	μ	F/Rm
		Uncracked Section		
4	1.00×10^{-3}	170.0		**
a	4.01×10^{-3}	42.4		1
12	9.03×10^{-3}	18.8		
16	1.61×10^{-2}	10.6		
20	2.51×10^{-2}	6.8	3	1.12
			10	1.23
24	3.61×10^{-2}	4.8	3	1.15
			10	1.12
28	4.92×10^{-2}	3.5	3	1.20
			10	1.33
32	6.42×10^{-2}	2.6	3	1.25
			10	1.47
		Cracked Section		
4	1.24×10^{-3}	137.1		
a	4.92×10^{-3}	34.2		1
12	1.12×10^{-2}	15.2		
16	1.99×10^{-2}	a.5	3	1.10
			10	1.20
20	3.11×10^{-2}	5.4	3	1.10
			10	1.30
24	4.48×10^{-2}	3.8	3	1.17
			10	1.36
28	6.09×10^{-2}	2.8	3	1.23
			10	1.47
32	7.96×10^{-2}	2.1	3	1.25
			10	1.70

* Participating Radius; since this is not well defined, a range of values is included.

** By observation, Pigure 2.26, "Introduction to Structural Dynamics" Riggs

TABLE 1-4

AVERAGE SHEAR STRESS - **CONTAINMENT**

Location ft.	Shear Perimeter ft.	Shear Area in^2	Reaction pounds	Average Shear Stress psi
15	32.6	14,474	**1,284,000**	89
19	37.0	16,428	**1,625,000**	**99**
27	41.8	18,559	**3,298,000**	178
35	50.2	22,288	**5,105,000**	229
41	99.8	44,311	**8,200,000**	**185***
50	45.5	20,202	**2,765,000**	**137**
58	49.2	21,844	**4,200,000**	**191**,+
65	49.2	21,844	686,000	32

SB 1 & 2 FSAR

*If the wings were assumed to have sheared-off at the time that the aircraft were crushing at this location the shear perimeter and reaction would-be reduced to 64.6 ft. and **6,070k** respectively. The average shear stress then becomes 198 psi.

If the horizontal and vertical stabilizers were assumed to have sheared-off at the time that the aircraft were crushing at this location the shear perimeter and reaction would be reduced to 42.1 ft. and **3,900k respectively. The average shear stress then becomes 209 psi.

+The average shear *stress* for the case were the crushing strength is reduced by 5 is 245 psi.

TABLE 1-5

COMPARISON OF ULTIMATE SHEAR STRENGTH CAPACITY*

Ultimate Shear Strength psi	Ultimate Shear Strength $\sqrt{f'c}$	Comment
717	13.1	equation 5-2, ϕ_o = .5
655	11.9	equation 5-1, ϕ_o = .5
607	11.08	equation S-10, ϕ_o = .5
527	9.62	equation 5-5, ϕ_o = .5
525	9.58	equation 5-2, ϕ_o = 1
523	9.55	equation 5-3, ϕ_o = .5
445	8.1	equation 5-1, ϕ_o = 1
391	7.14	equation S-10, ϕ_o = 1
383	6.99	equation 5-5, ϕ_o = 1
363	6.62	equation 5-12**
351	6.41	equation 5-4a
292	5.33	equation 5-6
219	4.00	equation 5-9, Committee 326 shear stress at distance d/2 from periphery ϕ = 1

*"The Shear Strength of Reinforced Concrete Member-Slabs", Joint ASCE-ACI Task Committee 426, Journal of the Structural Division, ASCE, Aug., 1974.

c = 93" $\sqrt{f'c}$ = 3,000 psi p = 0.0099

d = 37" f_y = 60,000 psi

**Adjusted for circular region, evaluated at d/2 away from periphery.

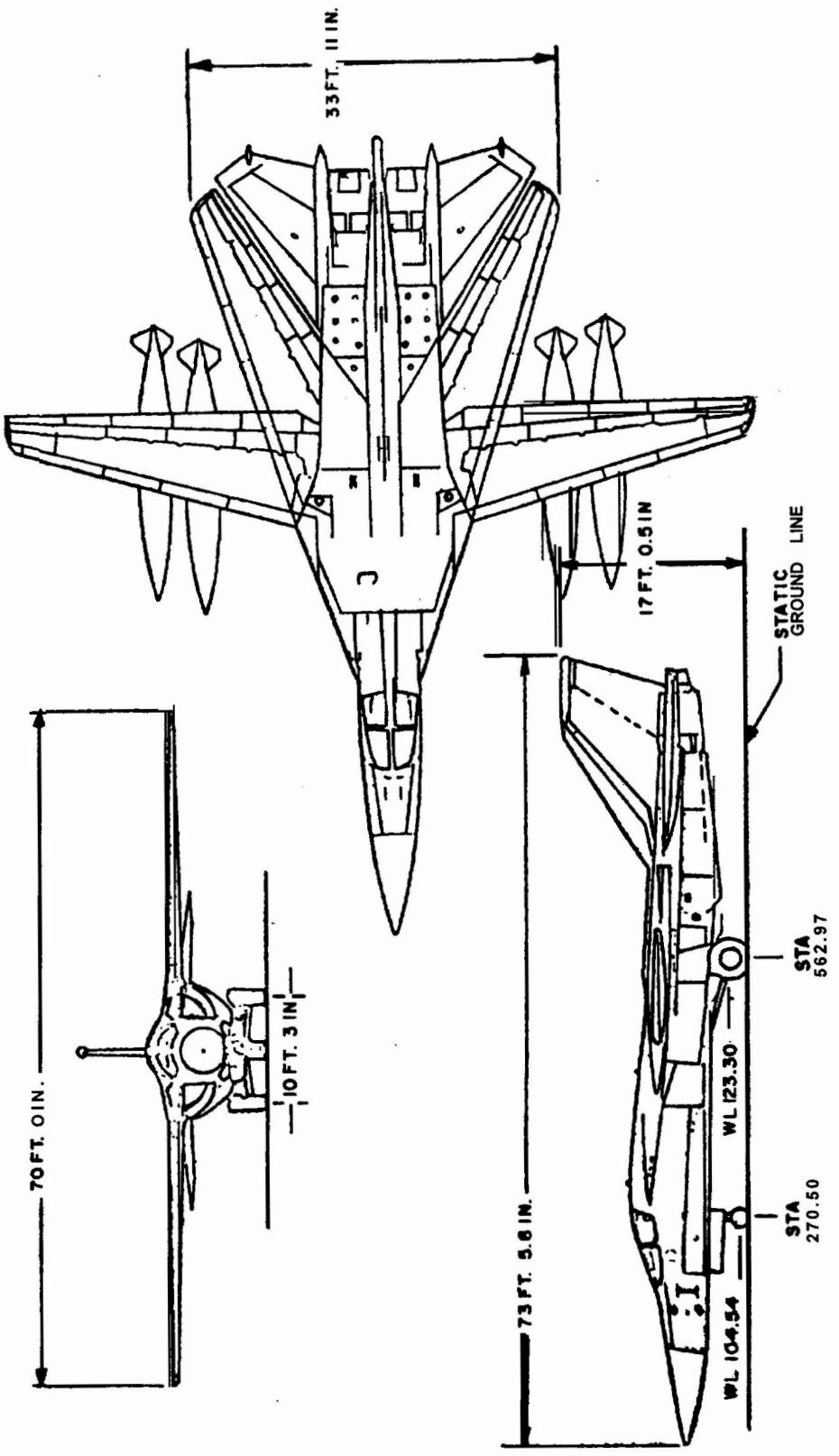

FIGURE 1

FB-111 CONFIGURATION (FROM REFERENCE 2)

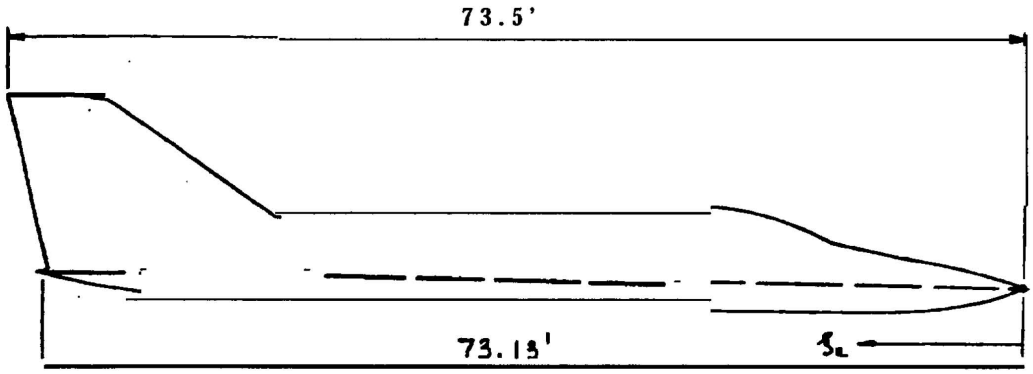

Figure 2A FB III • CONFIGURATION

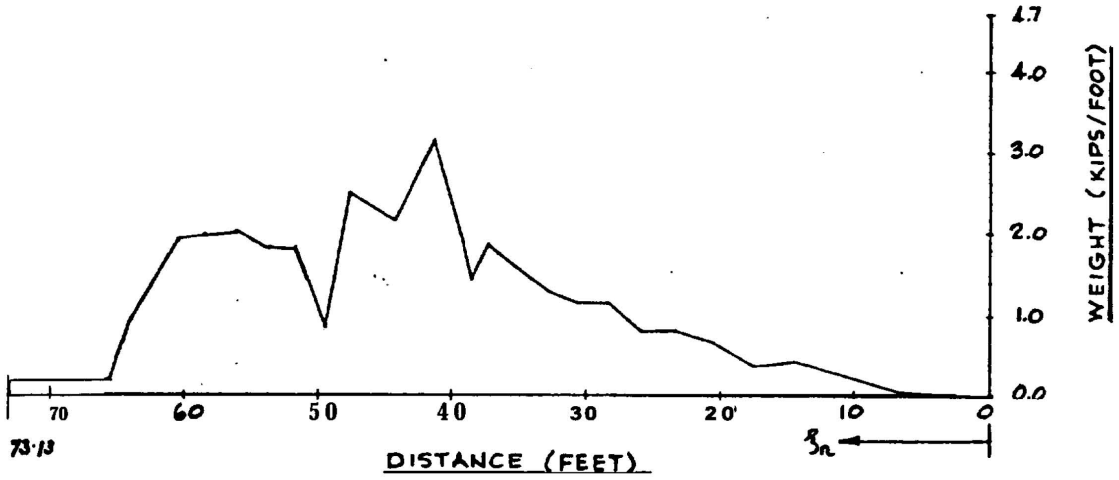

Figure 2B WEIGHT DISTRIBUTION

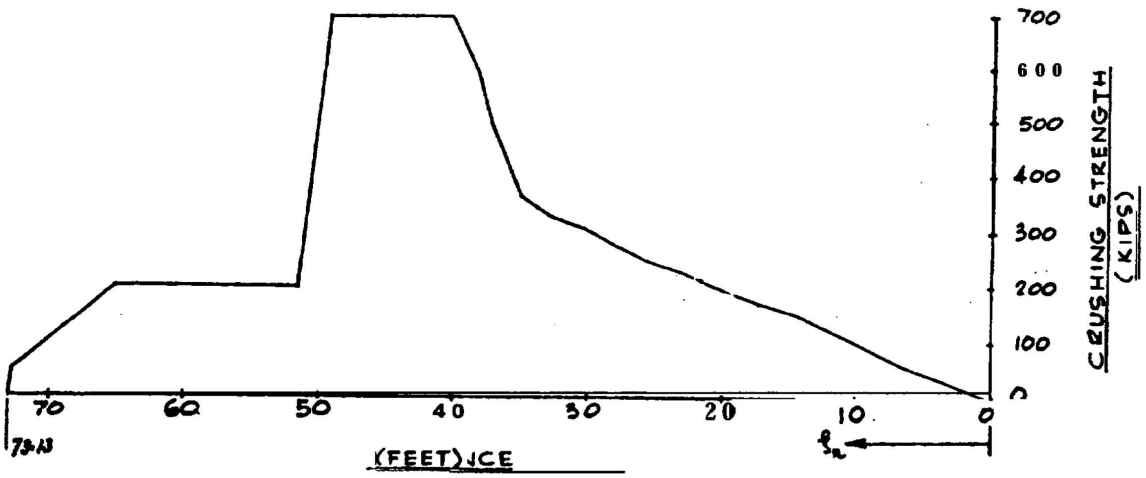

Figure 2C CRUSHING STRENGTH DISTRIBUTION

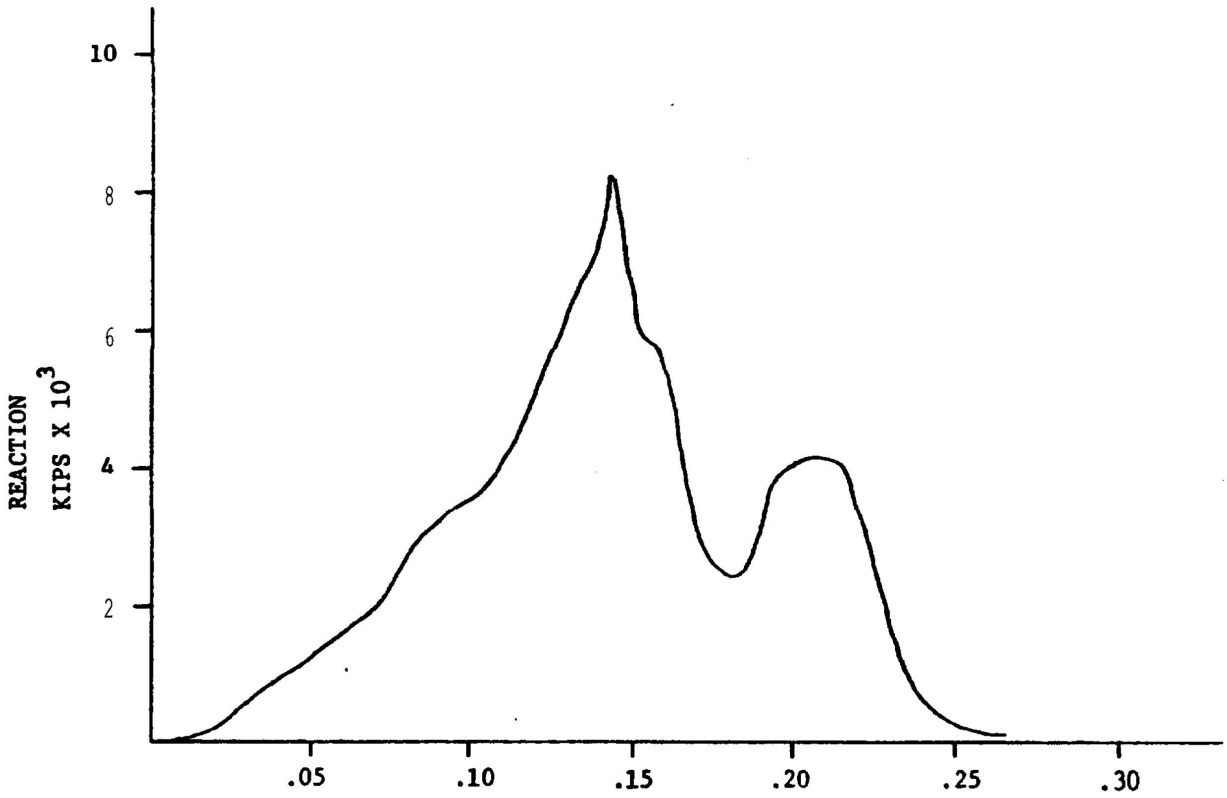

FIGURE 3

REACTION-TIME RELATIONSHIP

$P_c/5$ — — — —

$5P_c$ —·—·—·—·—

P_c denotes the scale crushing load used in the calculation. $P_c/5$ and $P \times 5$ denotes that one-fifth and five time the crushing load were used, respectively.

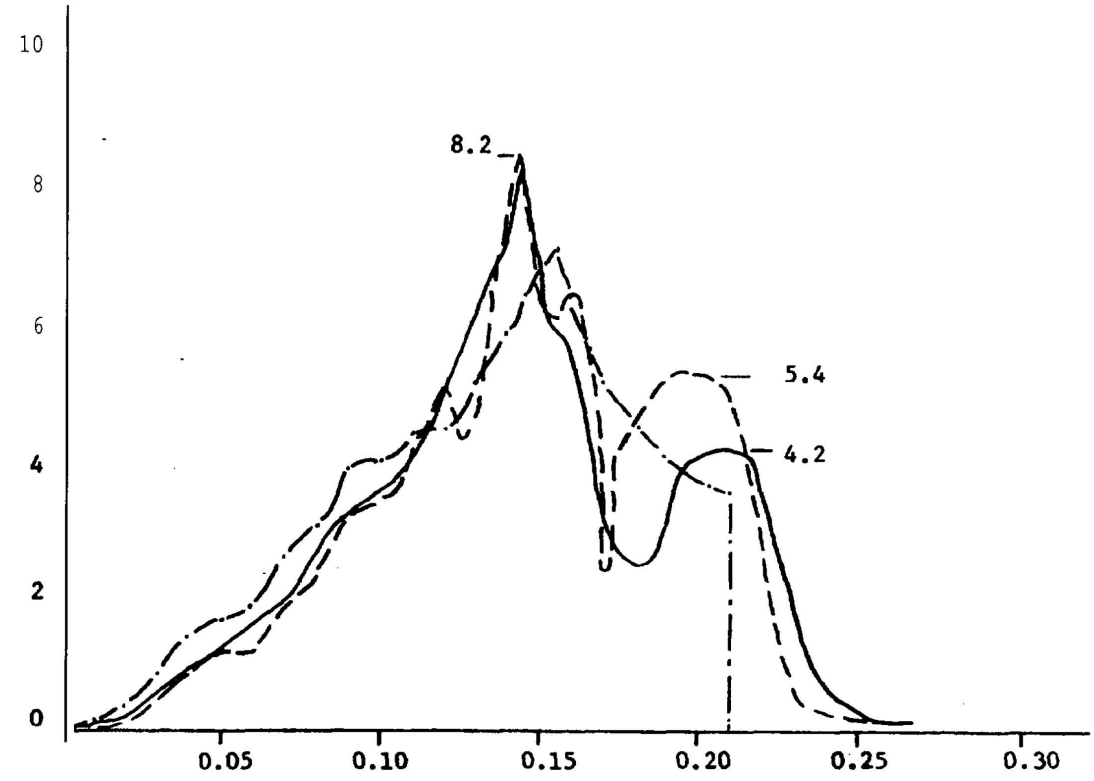

FIGURE 4

Reaction-Time Relationship for FB-111 with impact velocities of 200 mph.

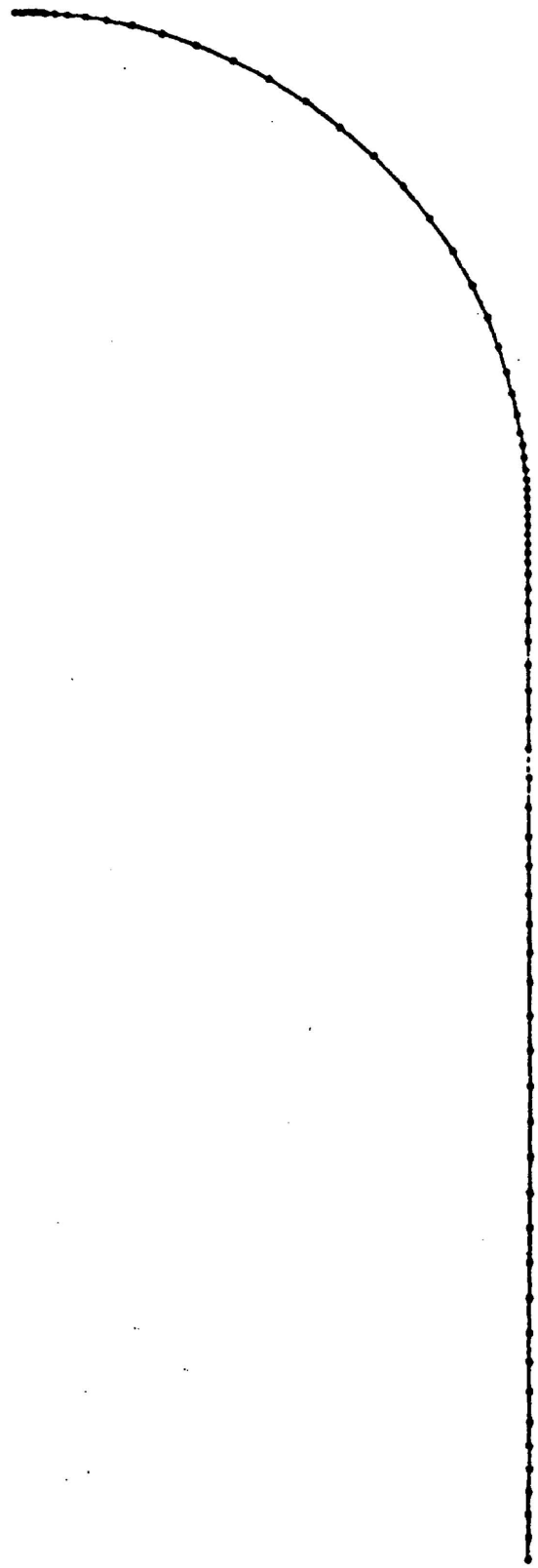

FIGURE 5
FINITE ELEMENT MODEL

PSNH SEABROOK S T A T I O N CONTAINMENT MISSILE IMPACT 6.1811 DEGREE IMPULSE

NO. OF COEFFS. 30.

MAXIMUM 3 .8909

MINIMUM -0.1382

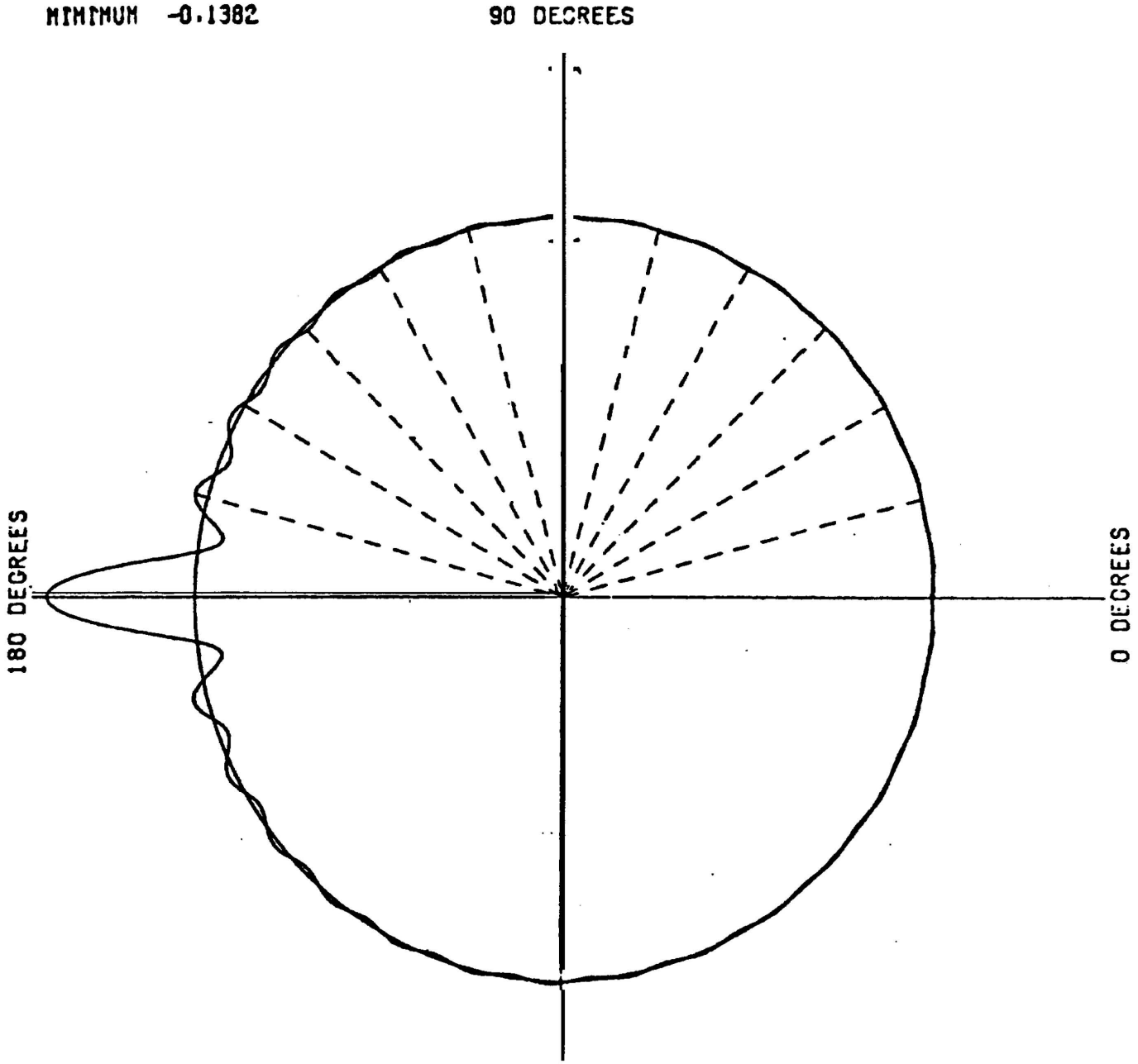

FIGURE.6
FOURIER SERIES REPRESENTATION OF SPRINGLINE LOADING

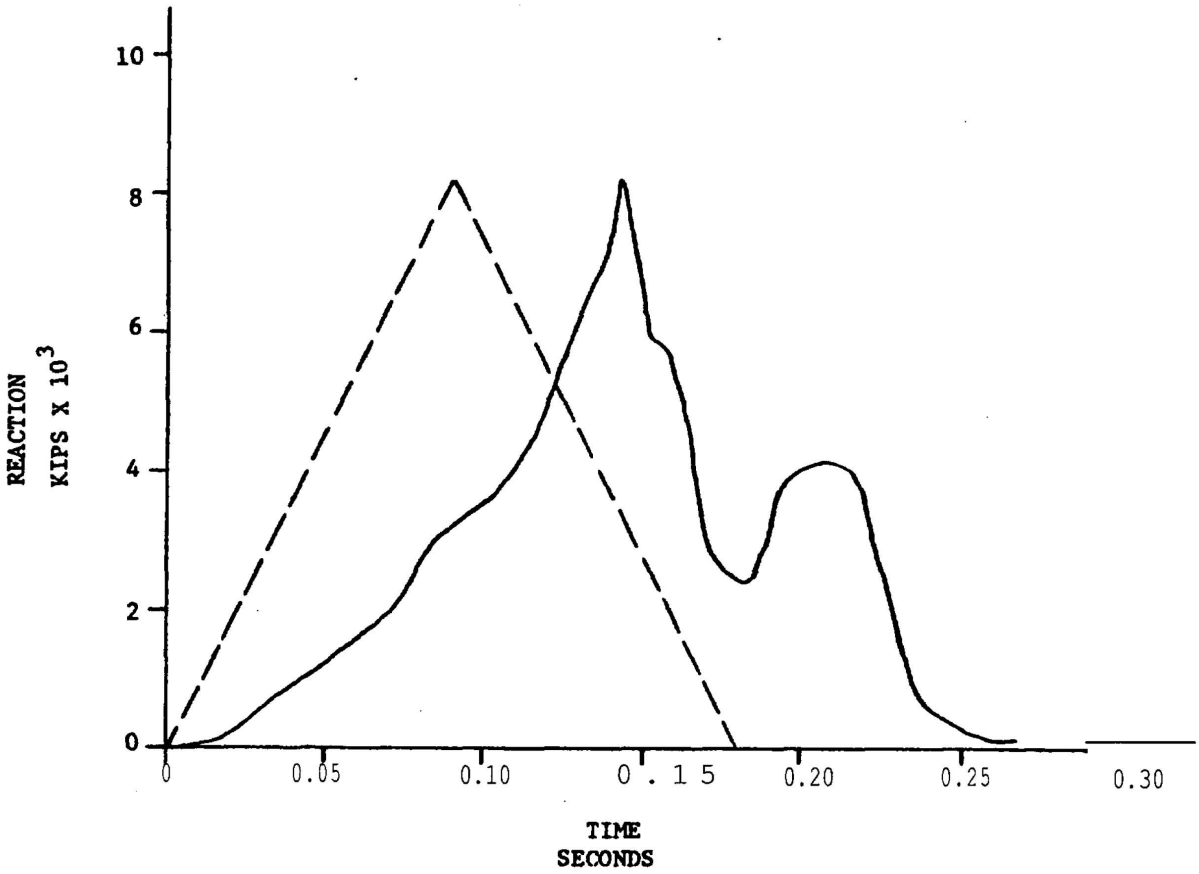

FIGURE 7 ACTUAL AND IDEAL REACTION TIME RELATIONSHIP

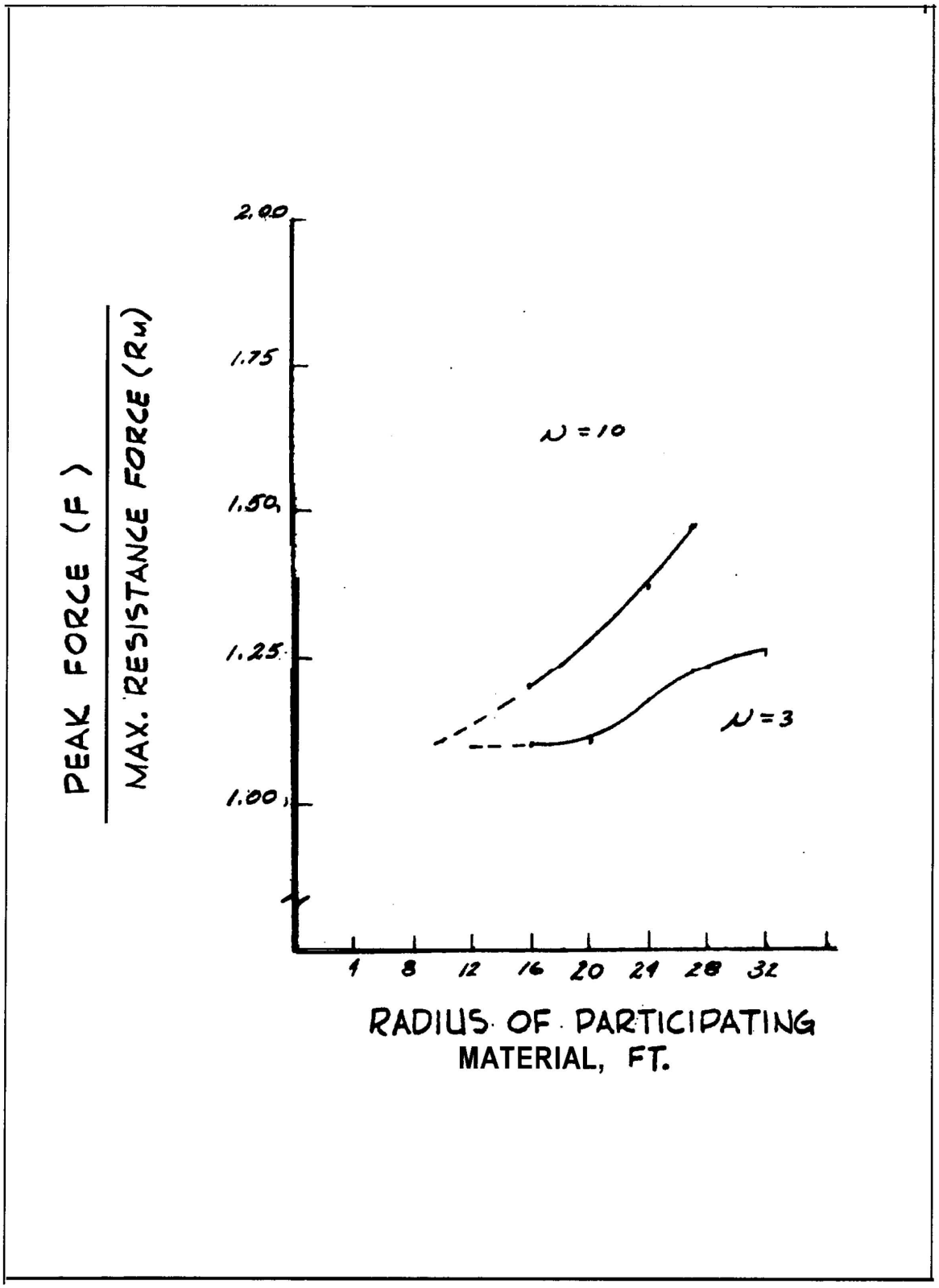

FIGURE 8
ALLOWABLE MAXIMUM FORCE, MAXIMUM RESISTANCE RATIO FOR VARIOUS DUCTILITY RATIOS AND PARTICIPATION TARGET MATERIAL RADII

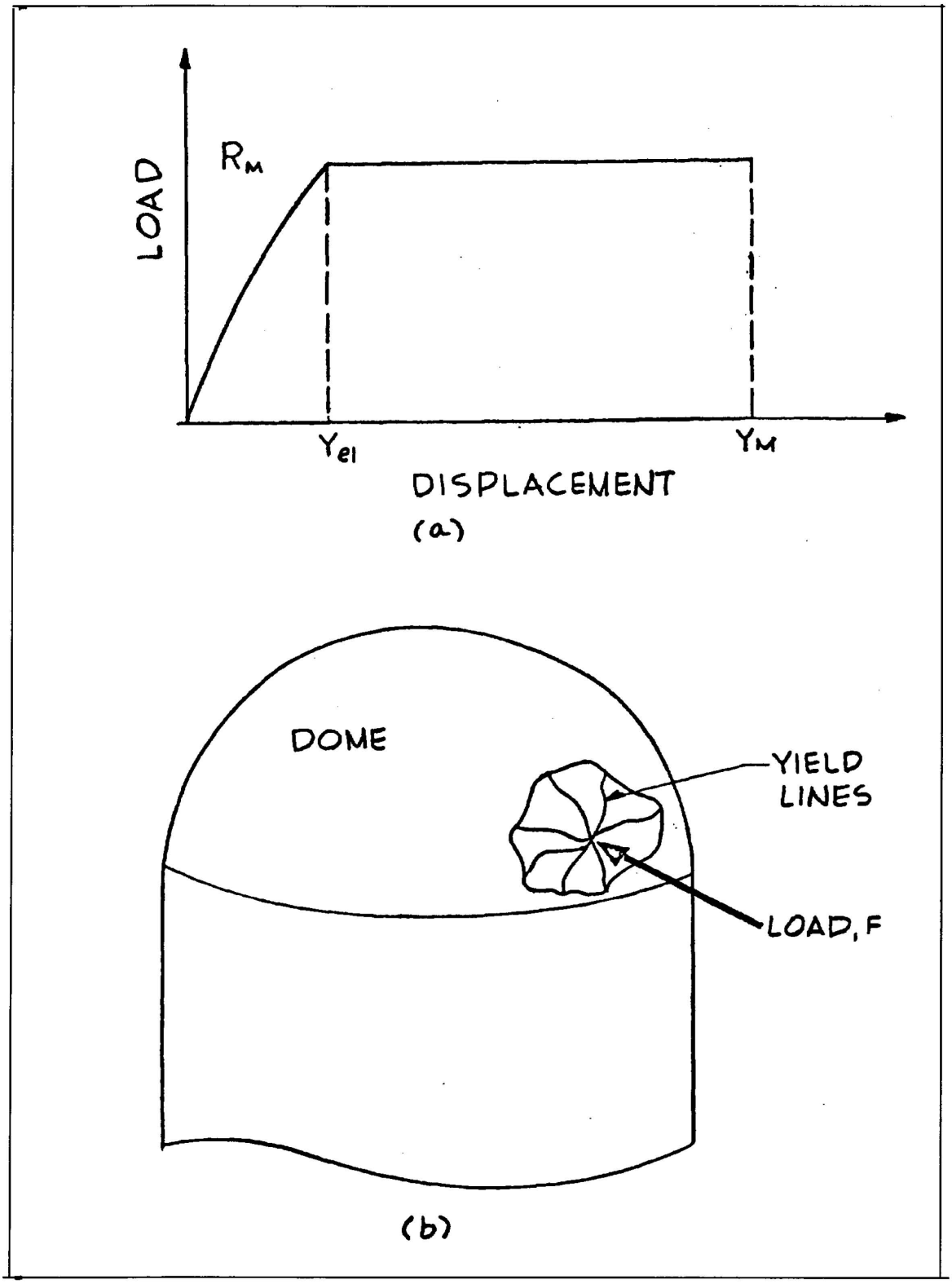

FIGURE 9

LOAD, DISPLACEMENT BEHAVIOR AND **POSTULATED YEILD** LINE CONFIGURATION

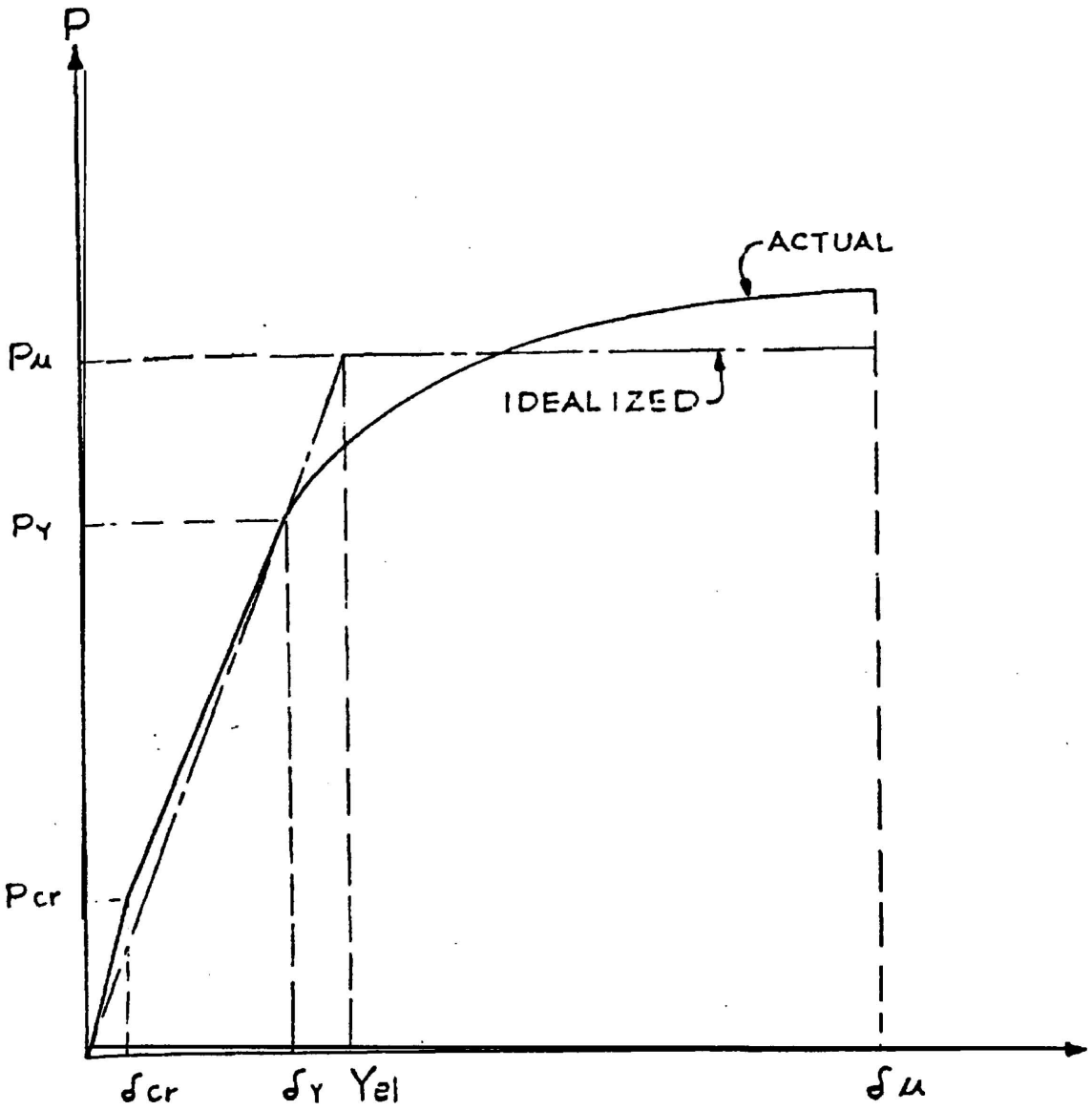

FIGURE 10.
LOAD-DISPLACEMENT CURVE FOR REINFORCED CONCRETE

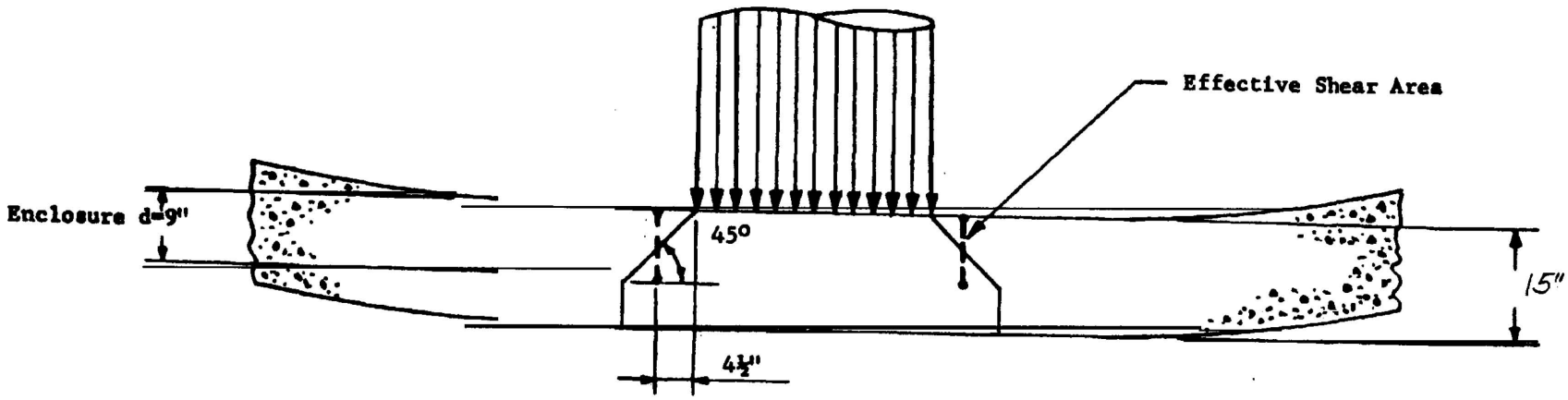

Figure 11, SCHEMATIC FOR EFFECTIVE SHEAR AREA - ENCLOSURE

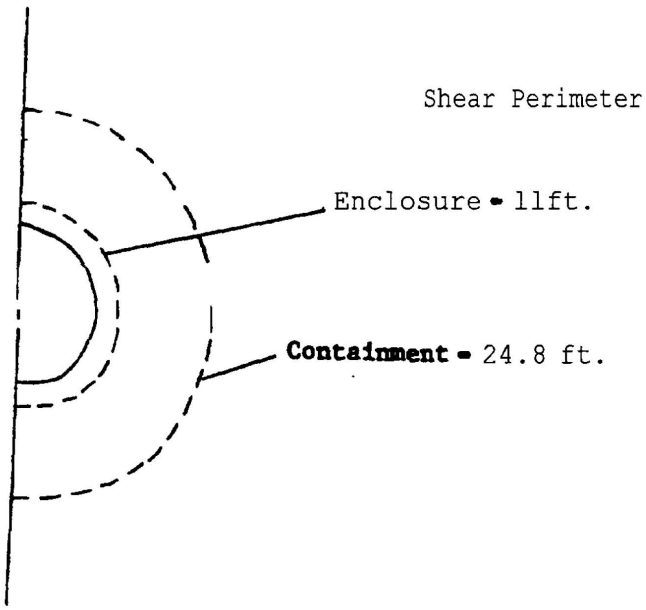

Figure 12 Impact Area and Shear Perimeter at 5 Feet From Nose

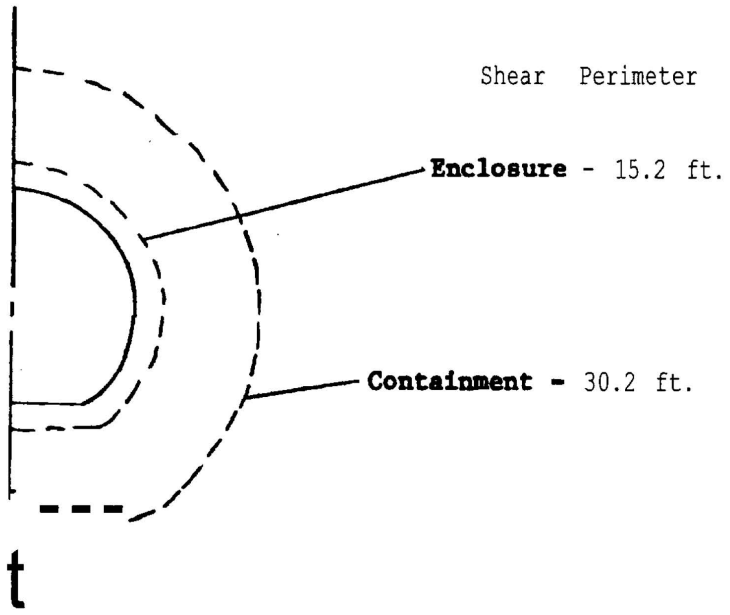

Figure 13, Impact Area and Shear Perimeter at 8.5 Feet From Nose

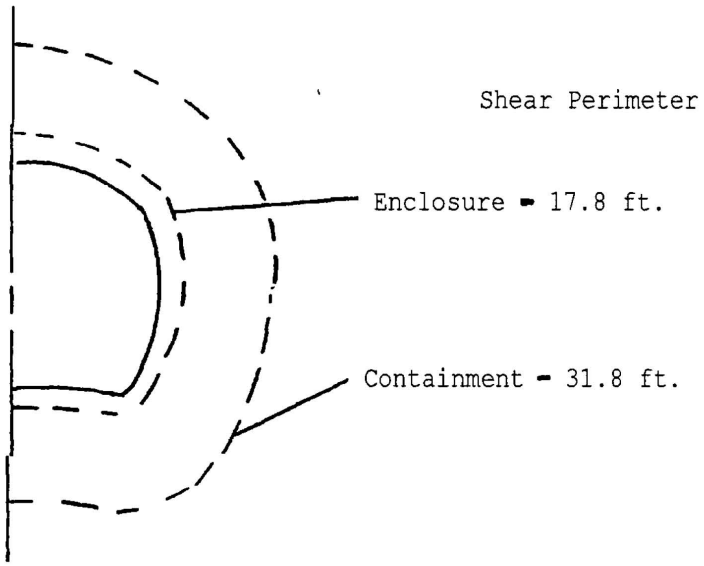

Figure 14, Impact Area and Shear Perimeter at 9.9 feet From Nose

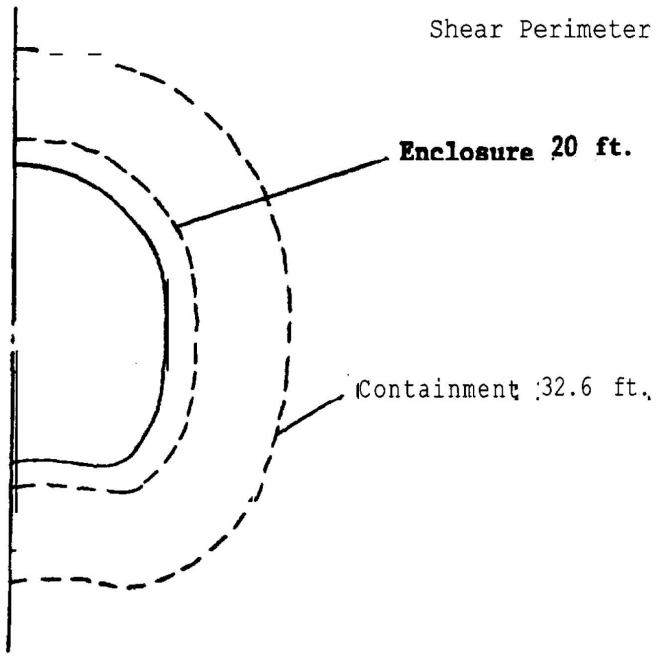

Figure 15 Impact Area and Shear Perimeter at 15 Feet From Nose

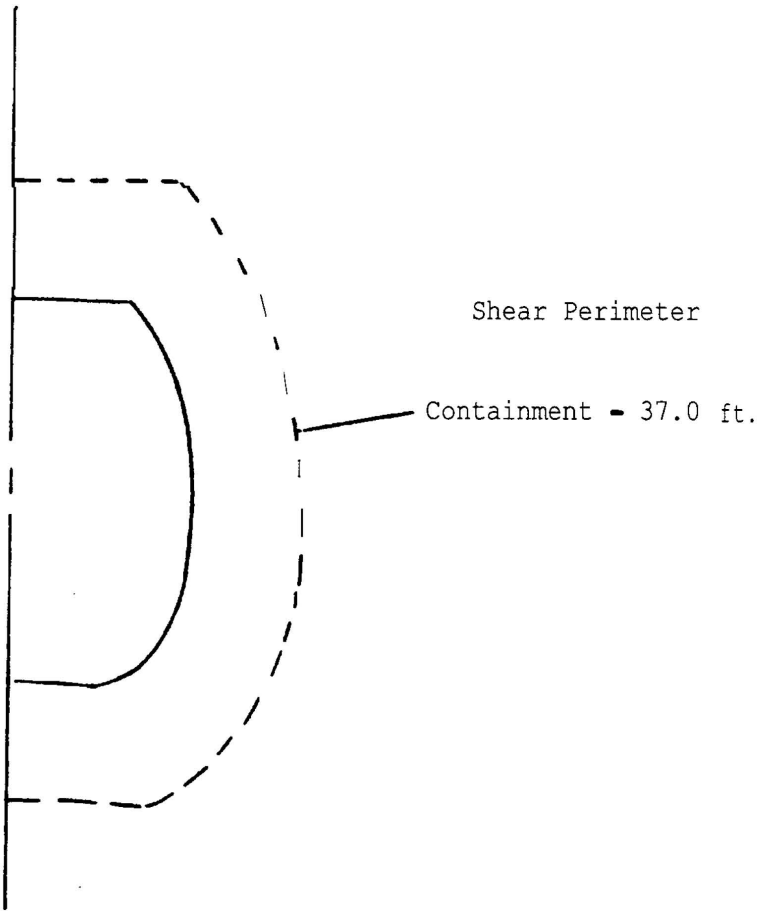

Figure 16, Impact Area and Shear Perimeter at 19.0 Feet From Nose

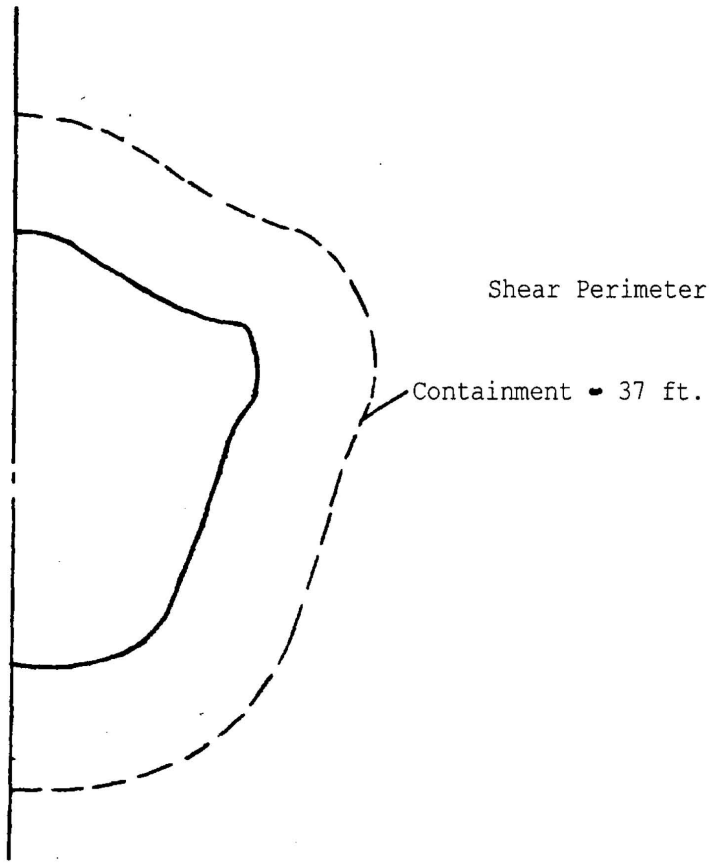

Figure 17, Impact Area and Shear Perimeter at 27 Feet From Nose

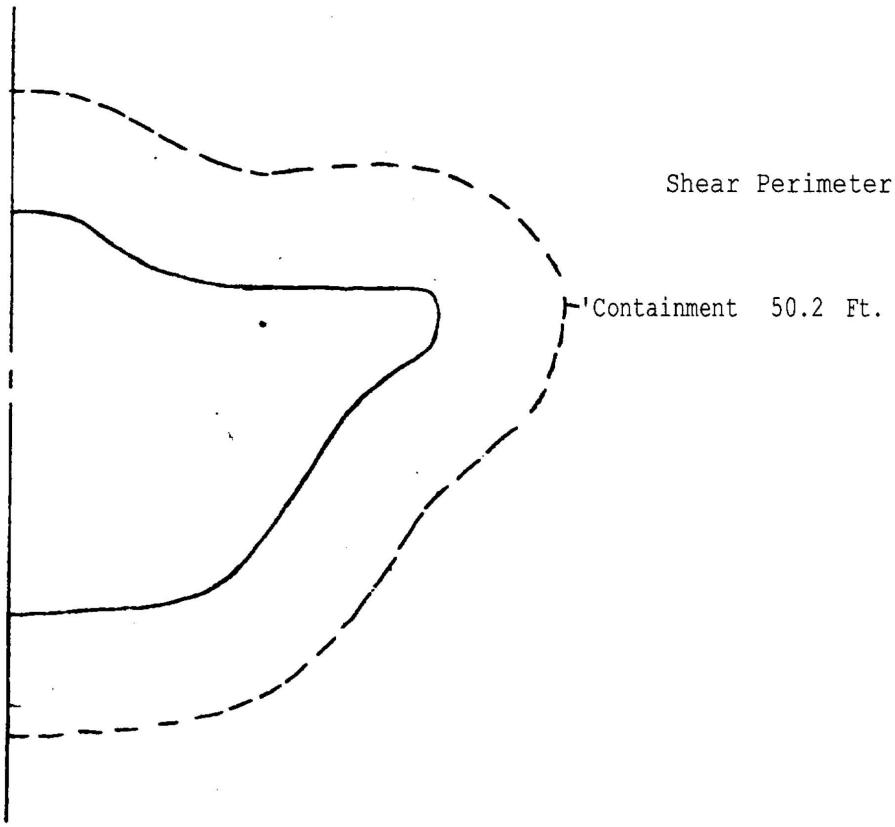

Figure 18 Impact Area and Shear Perimeter at 35 Feet from Nose

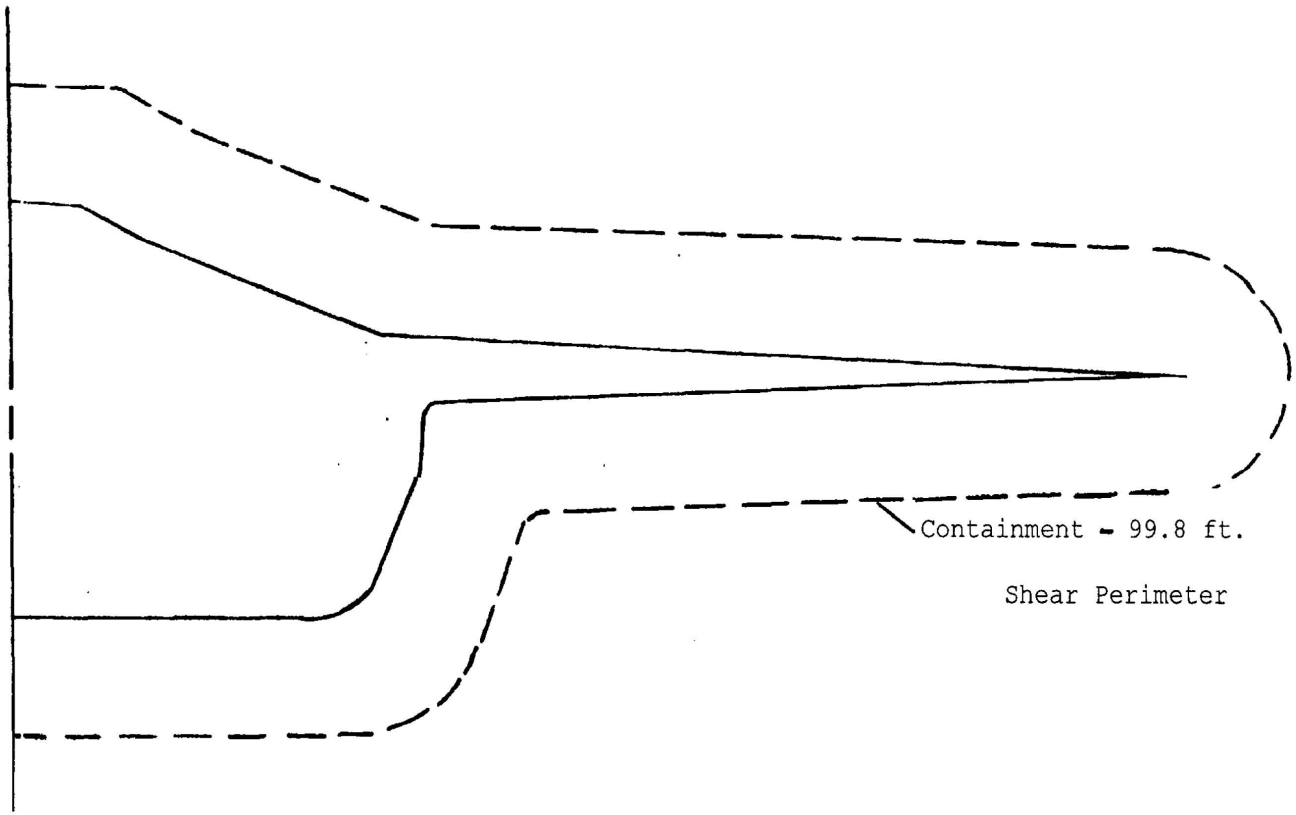

Figure **19,** Impact Area and Shear Perimeter at 41.0 Feet From Nose

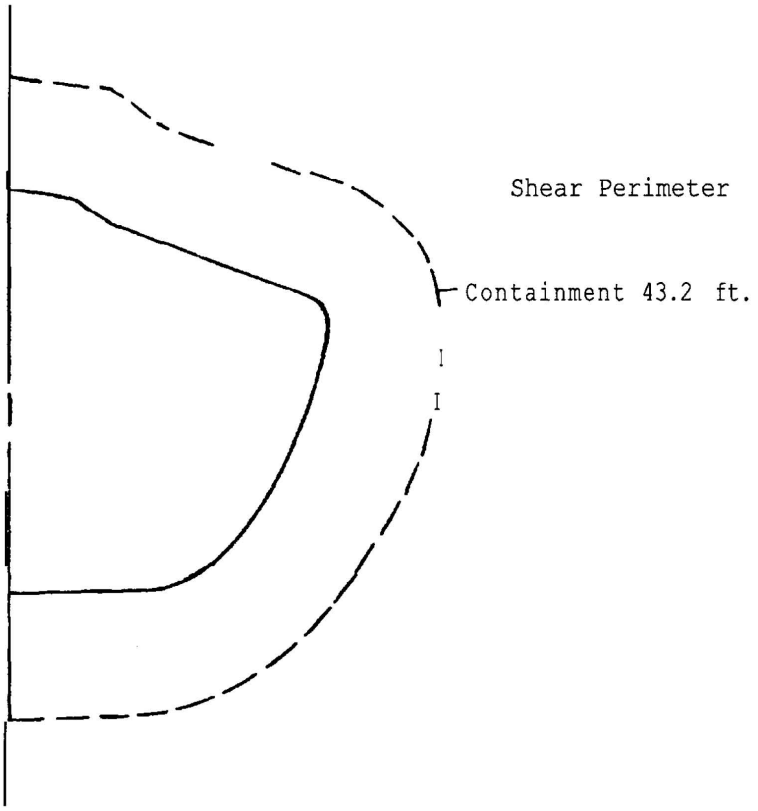

Figure 20, Impact Area and Shear Perimeter at 50.0 Feet From Nose

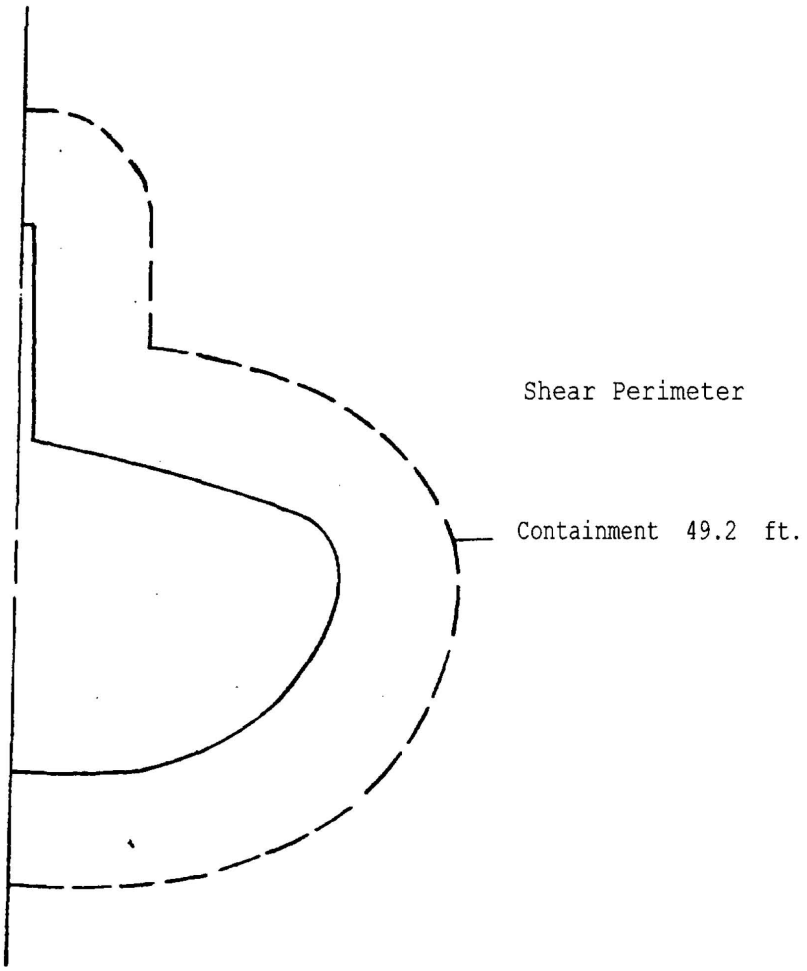

Figure 21 Impact Area and Shear Perimeter at 58.0 Feet From Nose

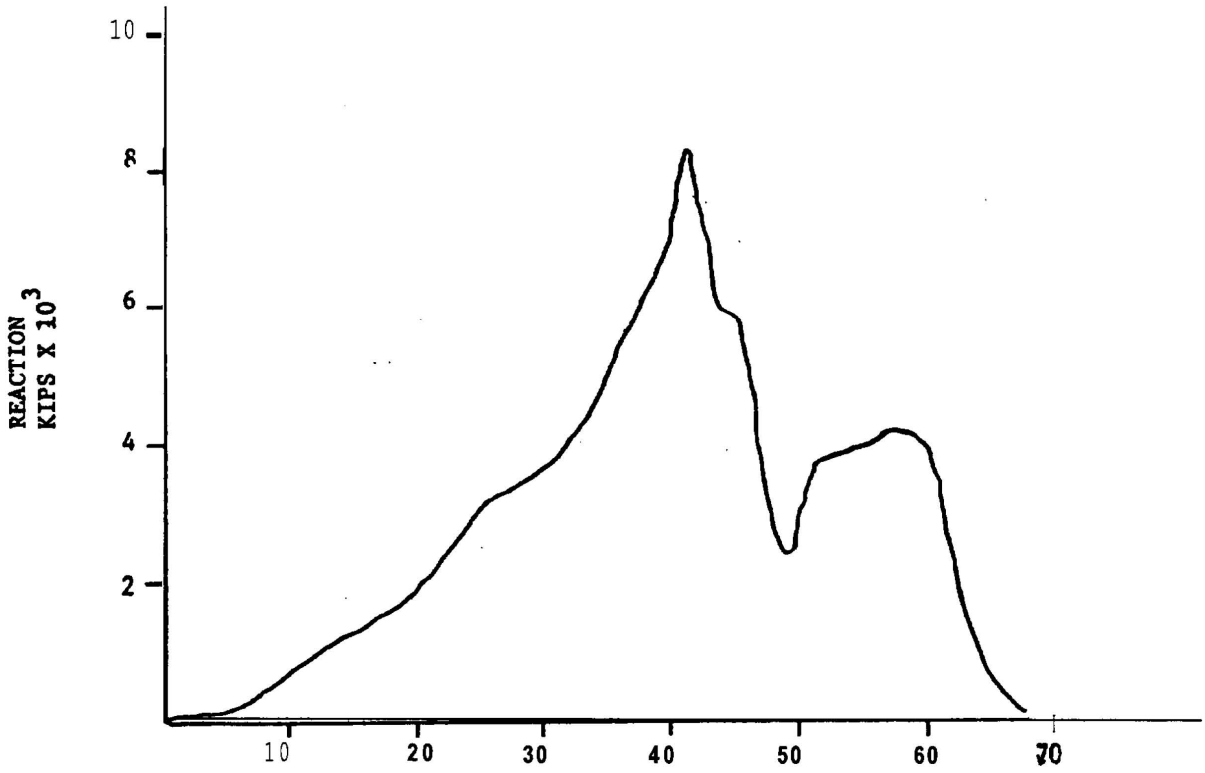

FIGURE 22, REACTION-CRUSHING LOCATION RELATIONSHIP

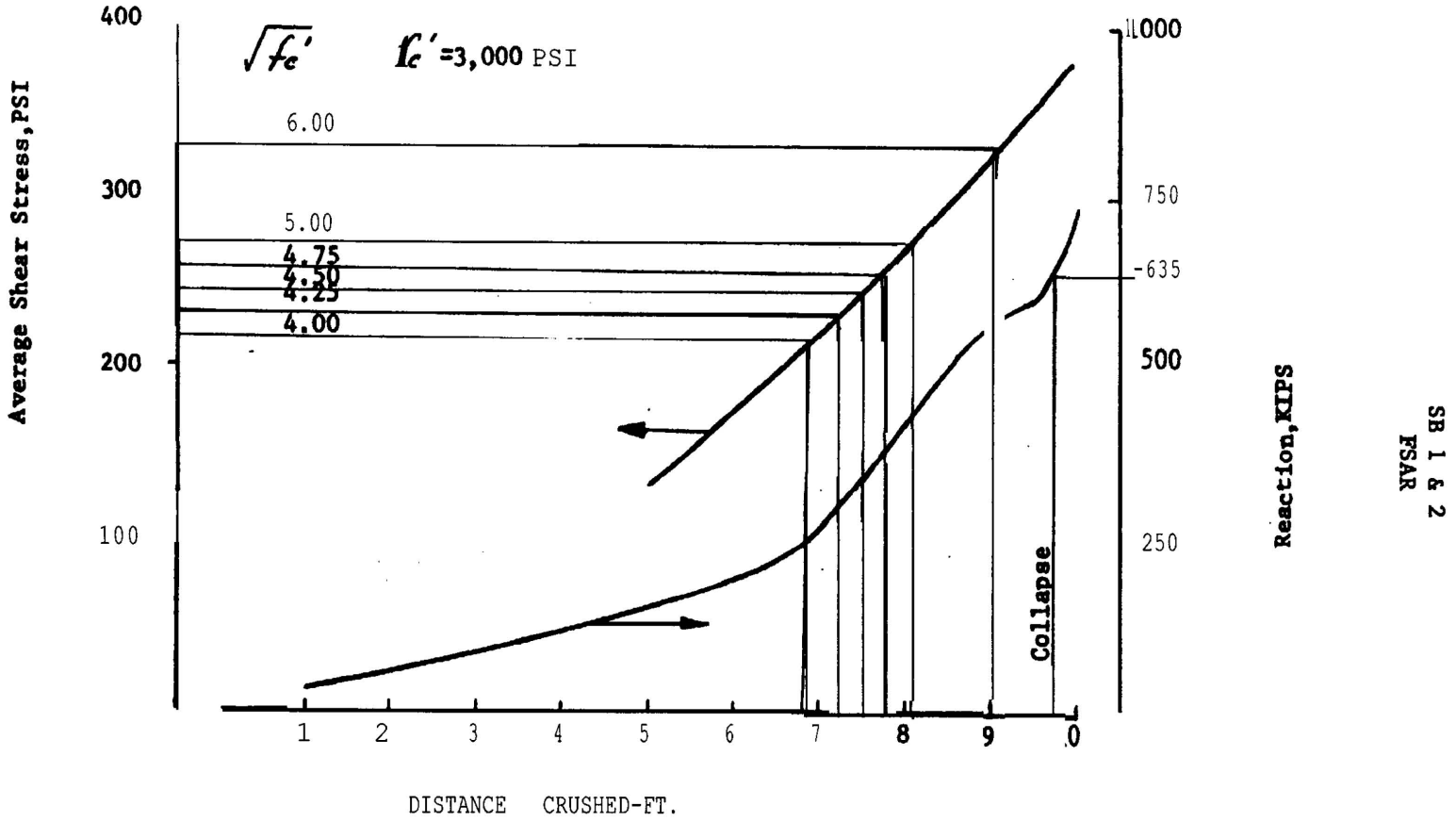

SB 1 & 2
FSAR

Figure 23 Average Shear Stress-Distance Crushed and Reaction Distance Crushed Relationship for the Enclosure Building.

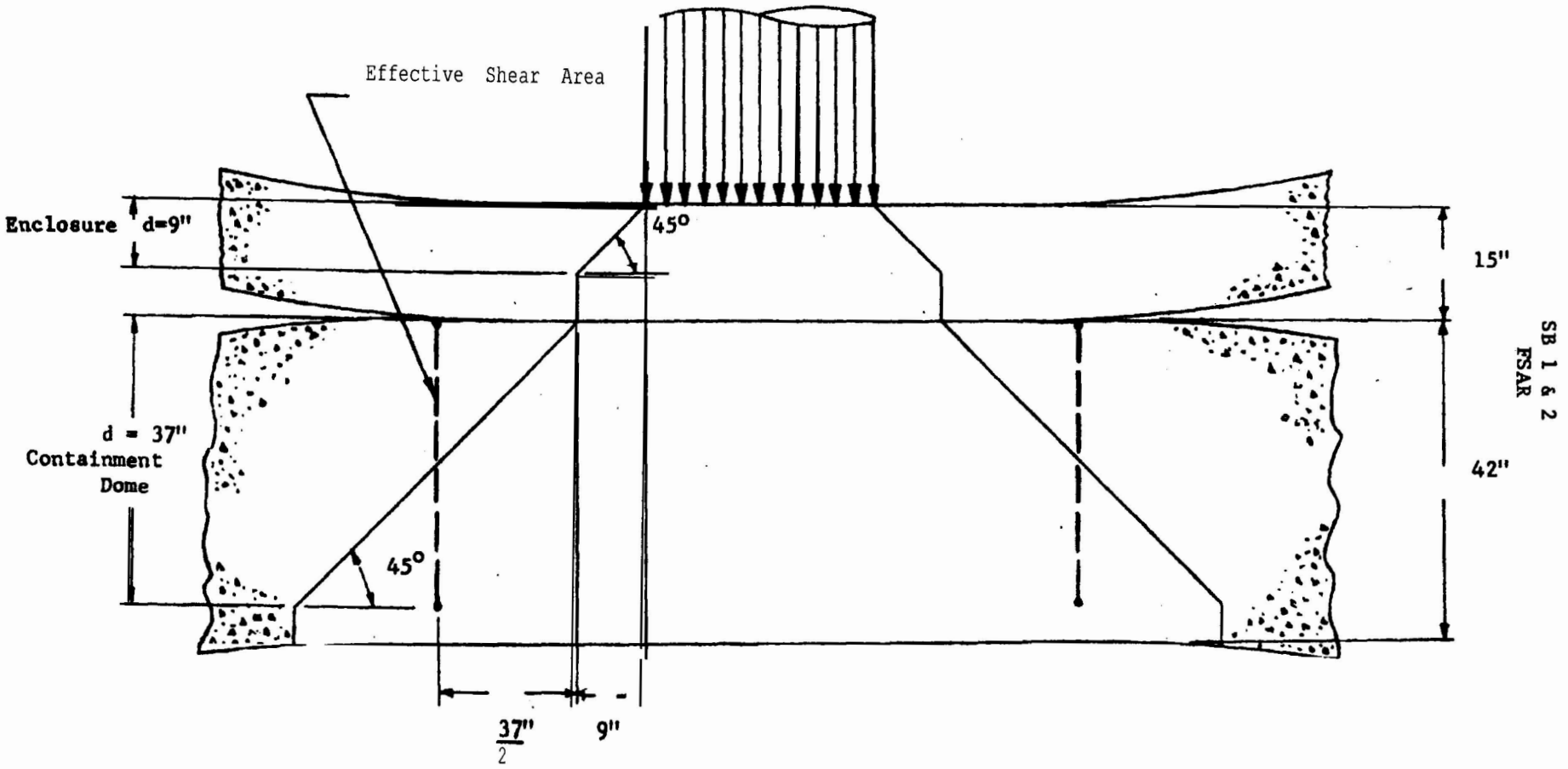

FIGURE 24 SCHEMATIC FOR EFFECTIVE SHEAR AREA - CONTAINMENT

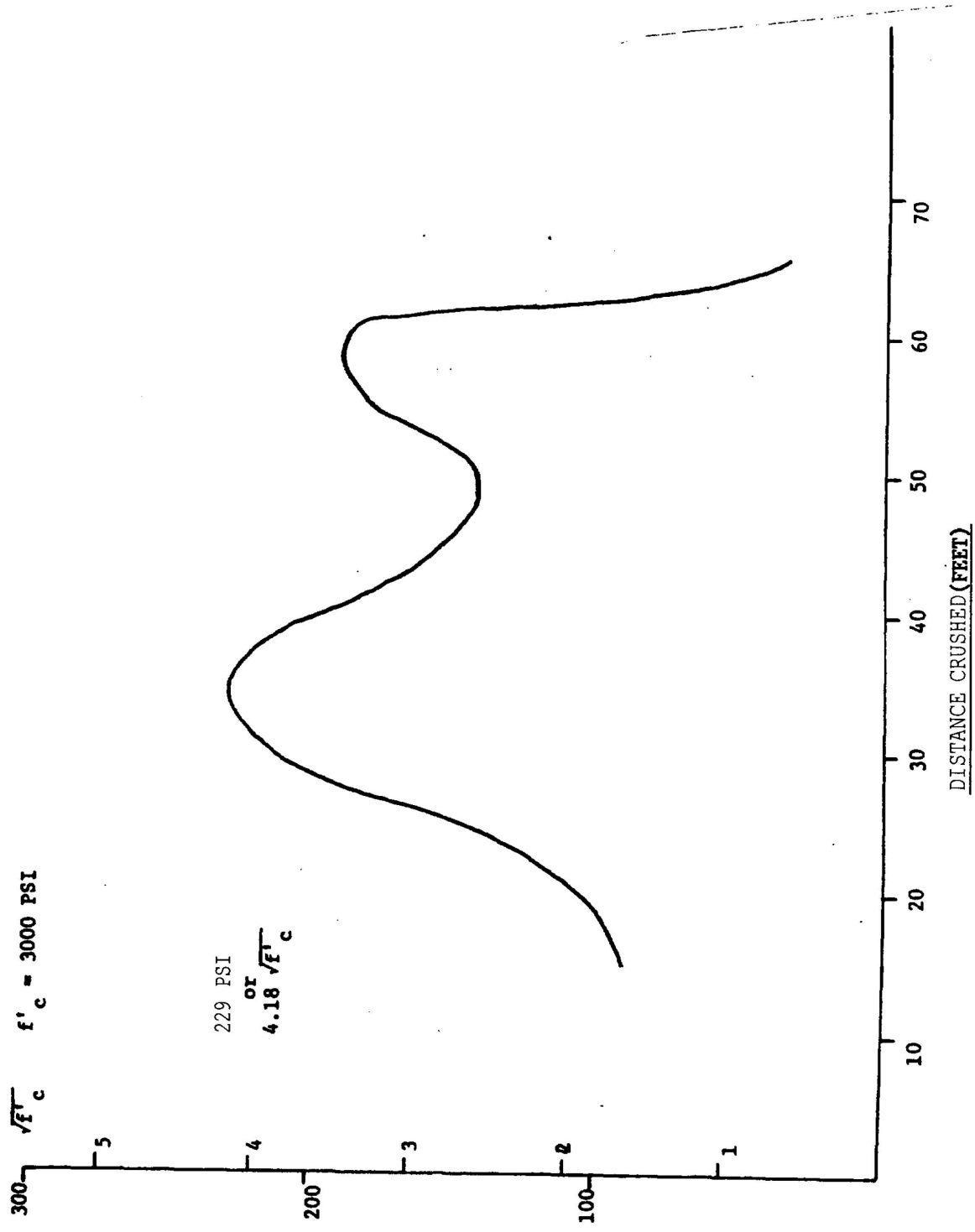

Figure 25 AVERAGE SHEAR STRESS-DISTANCE CRUSHED RELATIONSHIP FOR CONTAINMENT

2.0 FIRE HAZARD ANALYSIS OF SEABROOK STATION CONTAINMENT FOR AIRCRAFT IMPACT

A highly unlikely chain of adverse events is postulated in the following manner:

An FB-111 with a weight of 81,800 lbs and initial speed of 200 mph impacts on one of the two double containment complexes of the Seabrook plant. The enclosure building deforms locally under the initial impact, and the local deformation continues with little to no perforation until the enclosure building comes into contact with the containment building. This fact, plus the fact that if any penetration should occur it would be only the nose of the aircraft, will preclude the spilling of significant amounts of fuel into the annulus space. The annulus space contains no equipment, and all penetrations both mechanical and electrical are isolated from missiles and fuel by reinforced concrete slabs, The enclosure building acts as a barrier and directs the spilled fuel to the exterior area near the enclosure building. The following effects were then studied:

(1) Possible production of combustible vapor, its prompt ignition and the ensuing pressure pulse, and the possibility that the combustible vapor may be sucked into the plant areas and be cause for delayed ignition or toxic atmosphere in habitability systems.

(2) The fuel spilled and its transport to various areas of the plant. An ignition is then postulated, and the effect of the ensuing fire studied in order to evaluate

the safe shutdown capability of the plant.

(3) The effect of smoke and/or toxic gases as may be generated by the fire, with particular reference to control room habitability.

(4) The effects as detailed in (1) and (3) for all smaller aircraft.

2.1 COMBUSTIBLE VAPOR PRODUCTION

The FB-111 carries approximately 32,000 lbs of type JP-4 fuel. As indicated in Reference 1, the process of combustible vapor production is as follows: the crashing aircraft drags along the ground in a relatively slow deceleration (0.4 g) which lasts for a 'long' time (20 **secs),** and the fuel issuing from the wing after some postulated leakage mechanism is atomized to mist by the air as a result of its velocity relative to air. For the direct impact considered here,the decelerations are very high (peak value of 29 g) and of very 'short' duration (0.3 sec.). The atomizing process under these conditions is not significant. It is, therefore, concluded that the combustible vapor production and the associated hazards can be considered to be mitigated.

2.2 FIRE ANALYSIS

Various spill mechanisms are postulated either on the roofs or on the ground adjacent to the containment structure:

(a) The various roof areas adjacent to the containment enclosure with their elevation approximate areas, etc., are detailed in Table 2-1. As stated in PSAR Section 2.4, most of these roofs have parapets, and the roof drainage systems are designed to drain at least 3 inches per hour rain. It is

noted further that 1 inch of fuel takes 10 minutes to burn.[2] Using the minimum area in Table 2-1, and a catastrophic instantaneous mode of fuel release, the maximum expected duration of the fire is 17.9 minutes.

(b) For ground areas adjacent to the containment, there is approximately 1.5 acres of land, the total drainage of which is approximately 6 cfs. The spreading of the fuel over this area and the adequate drainage would result in a film fire with width comparable to the roughness of the pavement, e.g., 1/16 inch. The resulting fire would last only for 1 minute at the most.

(c) The mechanism of fire propagation was examined. No flammable material is normally expected to be present next to the containment which can serve as the propagator of the fire. The range of the fire has very conservatively estimated to be 200 ft. from its point of origin.

(d) Smoke is postulated to be traveling from this centre fire location carried by the wind. Its effect on the habitability systems was then studied.

(e) The possible hazard of fuel getting into the PAB Building through the vent stack is considered remote due to the following reasons:

a) The mechanism is improbable.

b) The entering fuel will be drained off at the base of the vertical stack, just as rainwater would be.

(f) The possible hazard of fuel getting into the main steam line tunnels through the side vent openings is considered not probable since the vent openings are above grade.

2.3 EVALUATION OF VARIOUS SAFETY RELATED AREAS

The various intake points to the safety related areas and their descriptions are detailed in Table 2-2, including the missile shields when applicable, under the accident conditions detailed in Subsection 2.3. All buildings other than the control room and the PAB residual heat removal area are either not needed for safe shutdown or are redundant. However, the conservative analysis below includes the reaction of these areas to the postulated fire.

(a) Control Room

There is no mechanism for the fire to endanger the habitability of the control room, since the split intake vents are at a distance of at least 300 ft. from the containment; therefore, it is beyond the reach of the direct fire. However, in the remote event that the fire finds its way into the intake structure, the temperature and smoke sensors will sense it and the intake opening will be closed. Under these conditions, the other intake will be used for ventilating the control rooms.

(b) Primary Auxiliary Building (PAB)

The air intake is located on the east wall of the primary auxiliary building at an elevation of 56'-0". The area in front of the intake has the containment enclosure roof elevation of 53'-0" and the east wall of the PAB faces the containment and the fuel storage building. There may be a small fire lasting 12.5 minutes at most on the roof of the containment enclosure area, a part of which may be injected into the PAB air intake, as its height is 3 ft. above the

roof of containment enclosure area. The inside of the PAB has roll-type filters after the intake and heating coil panels after the filter. Therefore, the flame and the hot gases would have to penetrate the filter and the coils before reaching the fans.

As indicated in Subsection 2.2, the roof surface of the containment enclosure area will be finished smooth and with proper drainage to drain off the spilled fuel quickly. Smoke and heat sensors will be located at the air inlet so that on a signal from them the operator can stop the fans.

(c) Diesel Generator Building

The diesel generator building intakes are on opposite sides of the building and are located at least 180 ft. from the containment structures. It is considered improbable that the spilled fuel will find its way underneath one of these intakes. Furthermore, the intakes are 28.5' above grade level, and it is unlikely that the fire will rise to that height. In addition, one of the intakes is shielded by the diesel generator building and it is thus not considered credible that the fire could reach that intake. Although it may be postulated that the hot gas from the direct intake point may cause momentary oxygen starvation of one diesel generator, the shielded intake will ensure the integrity of other diesel generator and of one train.

(d) Service Water Building

The intake for the service water building is approximately 280 ft. from the containment'and should be out of reach of the postulated fire. Furthermore, the air intake is located

in the east wall of the building. Consequently, the building serves as a shield for the spilled fuel flow. Additionally, there is a missile shield in front of the structure, which should inhibit any possible fuel flow and subsequent fire. The fire effects are, therefore, considered minimal. However, a minute amount of hot gas may enter the facility, but since the pumps are located at the west end of the building, it will not critically threaten their operation due to rise of temperature.

(e) Vent Stack

The vent stack is not a safety related item and, as indicated in Subsection 2.2, it does not furnish a significant pathway for the fuel to get into the primary auxiliary building. This mechanism of fire propagation is, therefore, considered incredible.

(f) Cable Spreading, Battery Room, Switch Gear Room and Cable Tunnel

The air intake for cable spreading, battery room, switch gear room and cable tunnel areas is through the mechanical equipment room of the diesel generator building, and the various safety aspects discussed for the diesel generator room hold for this case.

2.4 HAZARDS FROM SMALLER AIRCRAFT

The smaller plane crashes were examined for the various areas, as detailed in Subsections 2.2 and 2.3. The fuel in general may be JP-1, kerosene and JP-4. Since the fuel carrying capacity for all these planes is smaller than that of FB-111, and their burning temperatures are of the same order of magnitude, it was concluded that the effect would be enveloped by those in the case of FB-111.

2.5 CONCLUSIONS

In view of the results in Subsections 2.2 and 2.3, it was concluded that the hazard to Seabrook Station from direct fire after the postulated crash of an FB-111 or smaller aircrafts on the containment represents only very minimal potential hazard to the plant. The present design of the plant has inherent safety features so that the consequence of this minimal hazard is mitigated.

2.6 REFERENCES FOR SECTION 2

1. Appraisal of Fire Effects From Aircraft Crash at Zion Power Reactor Facility, I. Irving Pinkel, Consultant, Atomic Energy Commission, July 17, 1972.

2. Flammability Characteristics of Combustible *Gases* and Vapors, Bulletin 627, U. S. Bureau of Mines, 1965, Michael Zabetakis.

TABLE 2-1
ROOF DESCRIPTIONS

BUILDINGS	ROOF AREA (SQ. FT.)	ELEVATION	REMARKS
CONTAINMENT ENCLOSURE **AREA**	4,100	53' - 0"	WITH PARAPET
EMERGENCY FEED WATER PUMP BLDG.	3,000	47' - 0"	WITH PARAPET
FUEL STORAGE BUILDING	9,200	84' - 0"	WITH PARAPET
PRIMARY AUXILIARY BUILDING	8,144	81' - 0"	WITH PARAPET
PAB Filter Room	2,856	108' - 0"	WITH PARAPET

NOTE: GRADE ELEVATION 20' - 0"

TABLE 2-2

VENTILATION SYSTEM DESCRIPTIONS OF THE BUILDING SURROUNDING THE CONTAINMENT

SHEET 1 OF 2

BUILDING	BUILDING SURFACE FACING THE CONT.	LOCATIONS OF THE INTAKES			TYPE OF SHIELDING	REMARKS
		SURFACE	PATHWAY FROM CONT. WALL	ELEVATION		
Diesel Gen.	South wall	South Wall	200 ft.	28.5 ft. above gr.	Other Bldg. at 40' dist.	Ventilation & Combustion air; not necessary for safe shutdown.
		North Wall	240 ft. (thru roof)	28.5 ft. above gr.	Other Bldg. at 40' dist.	
PAB	East wall	East Wall	20 ft.	3 ft. above adjacent roof.	Shielded by the Cont. & F. Stg. Bldg.	Normal ventilation air; only RHR pump area safe shutdown related.
		North Wall	95 ft. (thru roof)	29 ft. above gr.	2' thick conc. missile shield.	Ventilation air to safety related primary component cooling water pump area and Boron injection pump area.
Emergency Feedwater Pump Bldg.	South Wall	North Wall	30 ft. (thru roof)	18 ft. above gr.	2' thick concrete missile shield	Ventilation air to the emergency feedwater pump area.

TABLE 2-2 (CONT.)
SHEET 1 OF 2

BUILDING	BUILDING SURFACE FACING THE CONT.	LOCATION OF THE INTAKES			TYPE OF SHIELDING	REMARKS
		SURFACE	PATHWAY FROM CONT. WALL	ELEVATION		
Service Water Pump House	West Wall	East Wall	290 ft. (t h r u roof)	45 ft. above gr.	2' thick conc. missile shield.	Ventilation air to the service water pump house.
		West Wall	180 ft.	13.5 ft. above gr.	2' thick conc. missile shield.	Air intake to the electrical areas.
Control Room & Computer Room	South 6 East Walls	Remote Intake Ports	300 ft. (at least)	At gr. level	Covered with grating.	Ventilation air to the habitable areas of the control and computer room.